Poly(3,4-ethylenedioxythiophene) in dye-sensitized solar cells: toward solid-state and platinum-free photovoltaics

ADVANCED SUSTAINABLE SYSTEMS
www.advsustainsys.com

Poly(3,4-ethylenedioxythiophene) in Dye-Sensitized Solar Cells: Toward Solid-State and Platinum-Free Photovoltaics

*Lucia Fagiolari, Erica Varaia, Nicole Mariotti, Matteo Bonomo, Claudia Barolo, and Federico Bella**

Dye-sensitized solar cells (DSSCs) have become a strong reality in the field of hybrid photovoltaics. Their ability to operate in diffused light conditions and the possibility of fabrication of modules bearing different colors make these cells attractive for different applications, for example, wearable electronics, building integration, etc. This review focuses on one of the compounds rather often studied for DSSCs, namely, poly(3,4-ethylenedioxythiophene) (PEDOT). It has been introduced both as a substitute for liquid electrolytes, in order to facilitate cells fabrication and increase their durability, and as an alternative to platinum for counter electrodes. The literature counts many studies on PEDOT and this manuscript collects them following a classification criterion based on applications, functionalization/doping strategies, and deposition methods. In addition to comparing the performance obtained for PEDOT-based systems with those of traditional cells (i.e., assembled with liquid iodine-based electrolytes and platinum cathodes), the manuscript also offers a brief analysis of costs and sustainability aspects, built up on experimental data found in the literature; this latter is expected to constitute a precious resource to catalyze the attention of the scientific community on relevant and preliminary aspects when figuring out the industrial scalability of newly proposed cell components.

1. Introduction

The scientific community agrees that photovoltaics (PV) represents the strategy capable of guaranteeing the production of energy in a geographically distributed way and without generating a considerable environmental impact.[1,2] Academic and industrial activities over the last 50 years have been very intense and today PV has become the cheapest source of energy in many countries (often costing less than 0.015 USD kWh^{-1}, i.e., 0.23 USD Wp^{-1}).[3,4] The leading technology on the market is that based on silicon and the production of solar panels has seen a significant decrease in manufacturing costs in the last decade.[5,6] Today, solar panels are placed in areas intended for electricity generation, integrated into buildings, on floating platforms, etc., and their diffusion is definitely growing.[7,8]

However, in this scenario some critical points are present, starting with the disposal of the panels at the end of their life and the need to integrate generation systems with storage units (given the intermittency of the solar source).[9,10] Nowadays, the scientific community is quite active in this direction and the numbers regarding energy production from PV are concretely promising.[11] Indeed, the International Energy Agency has recently predicted a growth by 700–880 GW from 2019 to 2024, that would make PV the technology with the largest installed capacity since 2025.[12] This well couples with another brilliant figure of merit, that is, the recovery of the manufacturing cost: right now, considering a rooftop PV system, this value is equal to 1.3 years in Canada, 0.9 years in Italy, and 0.4 years in India.[13,14]

Besides the evolution of Si-based market, other technologies have been developed, each of them for a specific application target or to propose a solution for one of Si-based cells issues.[15–19] Among these technologies, dye-sensitized solar cells (DSSCs) represent one of the most intriguing and scientifically stimulating challenges in the PV context.[20–22] 2021 will celebrate the 30th anniversary of their invention,[23] which has led to the generation of new knowledge in the field of molecular dyes, semiconductors and electrolytes formulations.[24–28] Their transition at an industrial scale was delayed for many years, and this was mainly due to the desire to consider DSSCs as alternatives to Si-based cells;[29] however, these technologies differ greatly in terms of materials, performance, costs and

Dr. L. Fagiolari, E. Varaia, Prof. F. Bella
Department of Applied Science and Technology
Politecnico di Torino
Corso Duca degli Abruzzi 24, Torino 10129, Italy
E-mail: federico.bella@polito.it
N. Mariotti, Dr. M. Bonomo, Prof. C. Barolo
Department of Chemistry
NIS Interdepartmental Centre and INSTM Reference Centre
Università degli Studi di Torino
Via Pietro Giuria 7, Torino 10125, Italy
Prof. C. Barolo
ICxT Interdepartmental Centre
Università degli Studi di Torino
Via Lungo Dora Siena 100, Torino 10153, Italy
Prof. F. Bella
National Interuniversity Consortium
of Material Science and Technology (INSTM)
Via Giuseppe Giusti 9, Firenze 50121, Italy

The ORCID identification number(s) for the author(s) of this article can be found under https://doi.org/10.1002/adsu.202100025.

DOI: 10.1002/adsu.202100025

end-of-life disposal.[30–34] In the last decade, the scientific community has focused the attention on the strengths of DSSCs, namely operation in diffused light conditions, the possibility of creating flexible devices and the tunable aesthetic aspect.[35–39] This has clearly led to the identification of commercially attractive products based on the DSSC technology, such as windows for buildings and colored panels for city/highway environments, self-powered wearable devices, smart objects for indoor environments being capable of producing energy, integrated energy conversion/storage devices, etc.[40–44] All these features make DSSCs complementary devices with respect to silicon in the PV scenario. Also, some companies have already started attending international conferences presenting prototypes, the industrialization of which is underway.[45]

DSSCs are considered as an emerging PV technology.[46] Their working principle is usually considered as an artificial photosynthesis in which a photon is converted into current instead of into a chemical species. A typical DSSC is based on a mesoporous semiconductor oxide, onto which a photosensitizer (acting as light catcher) is chemically bound; when the radiation shines onto the device, an electron is promoted from the highest occupied molecular orbital (HOMO) to the lowest unoccupied molecular orbital of the sensitizer and an exciton (i.e., a charge-hole separation) is created; this electron is then injected into the semiconductor and flows throughout the latter till it reaches the substrate and it is inserted into an external electric circuit; simultaneously, a redox mediator is employed to regenerate the steady state of the sensitizer by an electron transfer; in order to close the electronic (electric + ionic) circuit, the electron flows through the external circuit to the counter-electrode, where it is employed to regenerate the pristine state of the redox mediator.[21] Along with DSSCs, perovskite solar cells (PSCs) and organic PV belong to the emerging PV and the former one exhibits the best performance. However, PSCs are lead(II)-based halide perovskites and the presence of lead hampers the market acceptance.[47] Additionally, DSSCs could be easily integrated in building integrated PV (BIPV) projects (facades, green-houses, etc.) and could be effectively exploited in indoor applications or when diffuse light sources are required; indeed, PV conversion efficiencies (PCEs) up to 30% have been obtained in these conditions.[48,49] Also, they were recently exploited to power the Internet of Things.[50]

Among the open challenges in the DSSCs field, the removal of the liquid electrolyte and the replacement of the Pt-based cathode are the main ones,[51–55] as well as the most difficult. The goal is to increase the safety and ease of production of DSSCs (by replacing a liquid electrolyte based on organic solvents with a solid conduction system),[56–60] as well as to reduce the cost of the raw materials used for cells fabrication (by replacing platinum with less expensive alternative and carrying out accurate life cycle assessment—LCA—analysis).[61–65] The scientific community has proposed numerous solutions to these purposes, which are summarized in various reviews present in the literature.[66–70]

In this sector, poly(3,4-ethylenedioxythiophene) (PEDOT) plays an important role.[71] It was invented at the Bayer AG research laboratories around 40 years ago[72] and its excellent conductivity (300–500 S cm^{-1}), high flexibility, excellent transparency in visible light, remarkable stability, and low cost (even if an accurate and comparative LCA is still missing) make it among the most desired polymeric organic conductors of interest for electronic, antistatic and optoelectronic applications.[73–75] PEDOT is an insoluble polymer and it leads to difficult deposition processes from solution, but this issue was fixed by using a water-soluble polyelectrolyte, for example, poly(styrene sulfonic acid) (PSS), as the charge-balancing dopant during polymerization; as a result, PEDOT:PSS was obtained from the reaction.[76–78] The product of this important technical breakthrough (water processability) was sold as Baytron P™.

Wen and Xu illustrated two different synthetic routes to obtain PEDOT:PSS.[79] The first one involves the chemical oxidative polymerization of both PEDOT and PEDOT:PSS starting from 3,4-ethylenedioxythiophene (EDOT) monomer and poly(4-styrenesulfonic acid) (PSSH).[80] The final product is a metastable suspension obtained through a homogenization process. The second method involves an initial formation of PEDOT powder from EDOT and its subsequent dispersion in PSSH. Both the routes lead to PEDOT formation through an oxidative polymerization of EDOT monomer: the classical oxidizing agents employed are $FeCl_3$[80,81,92] and $Fe(OTs)_3$[80] along with $Na_2S_2O_8$.

EDOT monomer can be synthesized through different strategies (see **Figure 1**A).[82] The route suggested by Zhan et al. involves 3,4-dibromotiophene as starting material,[83] while Jonas et al. developed a synthetic pathway from thiodiglycolic acid, obtaining EDOT through the decarboxylation of 3,4-ethylenedioxythiophene-2,5-dicarboxylic acid.[84] In 2004, von Kieseritzky et al. obtained EDOT from 2,3-dimethoxy-1,3-butadiene.[85]

Besides the oxidative polymerization of EDOT, there are two further approaches to polymerize PEDOT: i) the electrochemical polymerization of EDOT and ii) the transition metal-mediated coupling of dihaloderivatives of EDOT. The former requires the use of small quantities of monomer and relatively short reaction time, while the latter gives the neutral polymer taking advantage of the dehalogenation-polycondensation method suggested by Yamamoto et al.[86–88] It is important to notice that PEDOT obtained through the oxidation method leads to p-doped polymers and the de-doping is not straightforward,[87] while the transition metal-mediated coupling leads to neutral polymers available for characterizations. However, the stable and easy-to-process PEDOT:PSS (Figure 1B) (that is water dispersible) is the preferable and most useful product.

PEDOT, PEDOT:PSS, and other doped PEDOT-based compounds have been widely investigated in the DSSCs field, with a double ambition, that is, replacing both the liquid electrolyte and the Pt-based cathode. Indeed, PEDOT-based materials can promote an efficient hole transporting (through a mechanism based on charge hopping) between cell electrodes, as well as an efficient electrocatalytic activity as cathodes in redox shuttles-based DSSCs.

This manuscript offers a literature review on the above mentioned two roles of PEDOT in the DSSCs field. The contents are presented according to a thematic overview based on the role and functionalization/formulation process applied to the PEDOT compound, also highlighting the relevant points in terms of cell performance (PCE, stability) and processability. Furthermore, we also present a section regarding the sustainability aspects and the industrial scalability issues of PEDOT

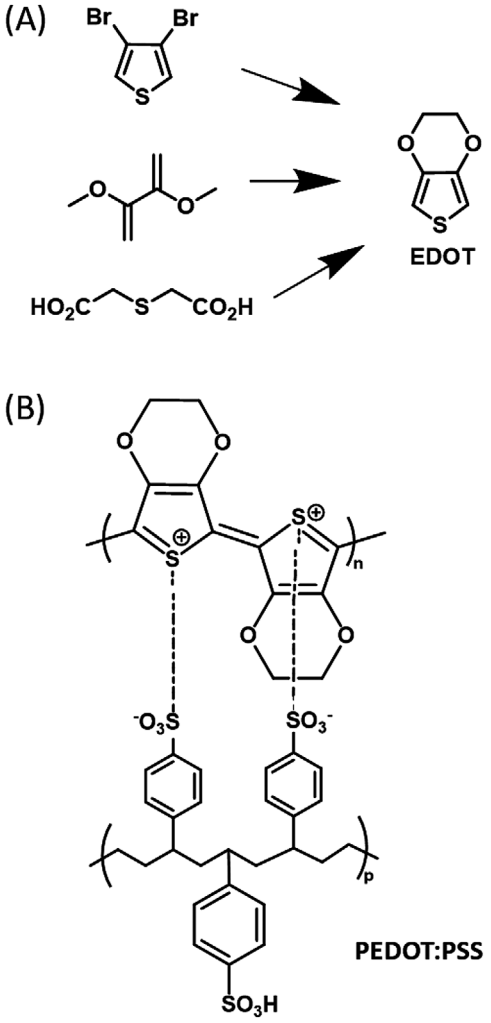

Figure 1. A) Three different starting compounds for EDOT synthesis, as presented in refs. [83–85]. B) Structure of PEDOT:PSS.

and PEDOT-based DSSCs, trying to check where the scientific community is placed within the transition process toward solid-state and/or Pt-free DSSCs. We can anticipate that in literature papers it is always claimed that PEDOT and PEDOT-based compounds would reduce the cost and/or the overall impact of the DSSC technology, but an accurate LCA study to consolidate this concept has not yet been carried out.

2. Current Trends and Challenges in Electrolytes and Cathodes for Dye-Sensitized Solar Cells

Although research efforts in the DSSCs field have been focused for many years on the development of new dyes with the aim of maximizing sunlight absorption and minimizing recombination phenomena,[89–91] the electrolyte has later come out due to its relevant role when long-term stability issues are considered.[92–94] In the standard device configuration, the electrolyte consists of a redox shuttle dissolved in an organic solvent along with additives conceived to boost photocurrent and voltage of the DSSC.[95,96] Overall, the electrolyte takes care of oxidized dye regeneration, a milestone step to make these solar cells regenerative, and guarantees an efficient charge transfer between the electrodes.[70] Last, but not least, electrolyte components should be designed to be easily upscaled at a large scale in terms of processability, abundancy and end-of-life disposal.[97]

Liquid-state electrolytes have been the first (and unique) choice in the DSSCs field for many years, due to their ability to ensure proper ionic conductivity and effective permeation throughout the nanostructured photoanode.[98,99] In terms of photoelectrochemical properties, the electrolyte must guarantee high stability under sunlight and cell voltage (≈1 V), while the redox shuttle potential has to be properly placed with respect to the HOMO level of the chemisorbed dye molecules to assure efficient sensitizer regeneration; other features include the best transparency as possible in the visible region (aiming at BIPV) and the low corrosiveness toward metal counter electrodes and charge collectors (long term stability).[100,101]

Redox shuttles based on iodine or cobalt represent the most studied systems for DSSCs electrolytes.[102] The former typically leads to fast dye regeneration, high ionic conductivity, and efficient permeation of the mesoporous photoanode: these features ensure an almost quantitative dye molecules regeneration.[103] However, iodine-based electrolytes have often been criticized for their corrosive action toward cell metals components;[104] other drawbacks are I_2 volatility, its competition with dye molecules for visible light absorption (due to I_3^-) and the overall high redox potential of this shuttle, that limits achievable open-circuit voltage (V_{oc}) values.[105]

As a valid alternative, Co-based organometallic complexes allow chemists to precisely tuning the electrochemical potential and optical properties of the redox mediator by designing different ligands around the metal center.[106,107] V_{oc} values close to 1 V were demonstrated by different groups, boosting the overall cell PCE in many cases.[108] However, these redox couples suffer of mass transportation issues due to their large molecular size, thus impacting on short-circuit current density (J_{sc}) values. Besides this, the scientific community is also considering the fact that cobalt is a critical raw material (CRM, with an abundance of 0.003% in the Earth crust and mined in few specific places); this implies that Co-based shuttles cannot be considered a winning solution for a large-scale diffusion of DSSCs.[109] In the recent years, some efforts have been spent on alternative redox mediators and the most promising are those based on copper complexes[110,111] and on sulfur-based compounds.[112] The former also led to solid-state devices, deriving from solvent evaporation, called zombie-cells.[113]

Solvent leakage, volatilization, and the ineffective sealing of liquid electrolytes-based DSSCs make these devices far from the long-term stability requirements for commercial purposes. This pushed the scientific community to develop quasi-solid electrolytes, that is, systems possessing—at the same time—the cohesive properties of a solid and the ionic conduction of a liquid.[114–116] Three main strategies are now established when proposing quasi-solid DSSCs: i) The solidification of a liquid electrolyte through an organic polymeric gelator, obtaining thermoplastic or thermosetting systems;[117,118] ii) the solidification of a liquid electrolyte by inorganic nanoparticles (NPs), leading to composite systems;[119] iii) the use of ionic liquids to replace organic solvents (and sometimes also the redox shuttle), with

the subsequent solidification with organic or inorganic gelators;[120] ionic liquids benefit from very low volatility and chemical stability, but their use is still controversial due to the often impactful synthesis. Overall, quasi-solid DSSCs have often demonstrated a promising long-term stability and rather high PCE values;[121–124] on the other hand, the permeation of these electrolytes in the whole thickness of nanostructured photoanodes has rarely been demonstrated, this latter representing a relevant pitfall in this field (i.e., only the first few layers would work in the TiO_2-based photoanode). If the upscalability of these electrolytes is further guaranteed by printing techniques, their use in commercial DSSCs could be reached within some years. In parallel, the scientific community is also studying the replacement of organic solvents with water, to fabricate both liquid and quasi-solid cells with a markedly improved safety and environmental friendliness.[125,126] Even if tailoring interfaces and cell components in water is a huge work under an experimental viewpoint, this will lead to a true concept of sustainable PV.[127]

In all the quasi-solid systems proposed right now, a liquid is still present and some criticism versus the unavoidable liquid exudation from the cells upon years is forcing a part of the scientific community to identify truly solid-state electrolytes.[69,128,129] The same criticism has been raised in the lithium batteries field.[130–135] Anyway, a first class of liquid-free systems is that of polyelectrolytes,[136] where charged anionic or cationic groups are chemically bonded to a macromolecular chain, leading the counterions to freely move between cell electrodes, undertaking charge carriers transportation. Besides polyelectrolytes, also plastic crystals (e.g., succinonitrile) were proposed as solid-state ion conductors.[137]

As a remarkable step forward, the redox shuttle can be completely replaced by a p-type semiconductor, working as hole-transporting material (HTM); in this system, charge transportation occurs by hole hopping between neighboring molecules or moieties.[138] This represents a typical electronic transport, markedly different from the ions-based conduction where mass transportation is required. Among the requirements of HTMs, the main ones are the deposition in the amorphous state within the mesoporous photoanodes (to guarantee an efficient pore filling), a high hole mobility and a wide transparency in the visible range. Cu-based compounds (e.g., CuI, CuBr, CuSCN) were demonstrated to this scope in DSSCs, and the best performances were obtained with the orthorhombic perovskite polymorph of $CsSnI_3$, able to reach PCE higher than 10%.[139]

As regards organic HTMs, they are polymers or molecules soluble or dispersible in organic solvents, thus spin-coating can be used for simple lab-scale preparation;[140] anyway, in situ formation by means of electrochemical or photo(electro) chemical polymerization methods were also proposed.[141] PEDOT, poly(aniline), poly(3-hexylthiophene), poly(3-octylthiophene), polycarbazoles, triarylamine-based polymers, and poly(thiophene) represent the most frequently used polymeric HTMs in solid-state DSSCs.[142] As regards molecular compounds, 2,2′,7,7′-tetrakis(*N*,*N*-di-p-methoxyphenylamine)-9,9′-spirobifluorene (spiro-MeOTAD) represents the main choice nowadays,[143] even if it is rather expensive and requires precise doping conditions to properly work in DSSCs.

Even if these solid-state systems guarantee the absence of any leakage or volatilization phenomena, state-of-art performances are still far from those achieved with liquid electrolytes. The main issue of HTMs is the poor interfacial contact with cell electrodes and permeation throughout the mesoscopic structure of the photoelectrode; these characteristics are of fundamental importance for hybrid PV technologies. Many efforts are currently spent to make steps forward developing HTMs-based DSSCs.

A list of the principal keywords representing the state-of-art research in the field of DSSCs electrolytes is shown in **Figure 2**.

Counter electrodes (or cathodes in n-type cells) are a key component in DSSCs, working not only as a charge collector, but also playing an active role in the efficient regeneration of the redox mediator. Since the seminal work of O'Regan and Grätzel,[23] counter electrodes are commonly made of platinum. Albeit this metal shows an excellent catalytic activity (especially toward the classical I-based redox couple), it presents some important drawbacks both concerning costs, device scalability and environmental issues, being it considered as a CRM.[144] Therefore, the research started to focus on alternative materials that should, however, fulfil some key requirements: They should i) be catalytically active toward a selected redox pair; ii) be obtained in thin films with large surface area to increase the electrode/electrolyte interface; iii) be chemically, thermally, and physically stable; iv) be CRMs-free and obtainable by means of

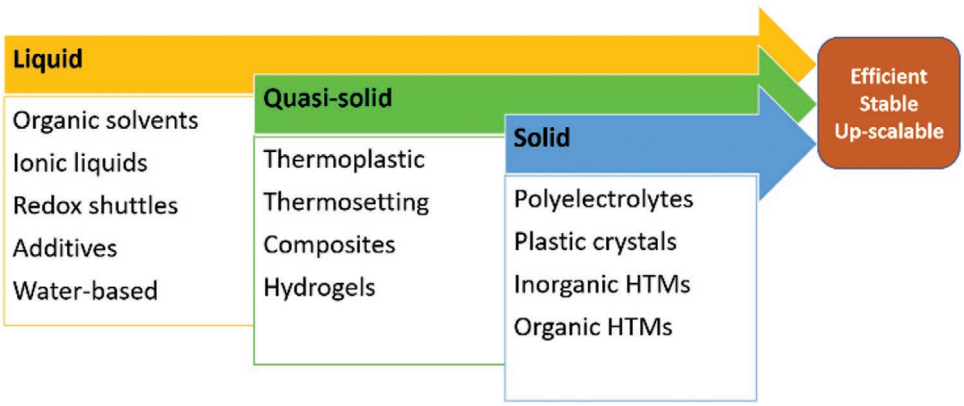

Figure 2. Main keywords of current research efforts in the development of electrolytes for DSSCs.

cheap and easy approaches. Additionally, some other properties are requested for specific application such as high transparency or the ability of standing on plastic substrates for BIVP, wearable electronics and indoor application.

Aiming at replacing platinum, but keeping high PV performances, several materials have been exploited, and can be categorized in two main classes: transition metals-based (inorganic) compounds and carbonaceous materials. The former class could be further divided in oxides, sulfides, and selenides,[145,146] whereas the latter includes different inorganic C-based compounds.[147–149] Given to the topic of the present review (i.e., PEDOT-based materials), a detailed description of different compounds developed and tested as Pt-free counter electrodes falls outside the scope of this work. Albeit a general description of the principal employed materials is proposed hereafter, the reader is kindly addressed so some accurate reviews giving an exhaustive overview on the topic.[150–152] Moreover, throughout this section, we limit our analysis to liquid-based DSSCs.

Indeed, to pick the best Pt-free counter electrode is not an easy (but somehow interesting) task, being the final application of the DSSC of pivotal importance to drive the selection. Additionally, the most interesting cathodes should be thoughtful chosen considering the redox couple to be coupled with. Yet, some advantages or issues related to each material could be drawn. Starting from carbonaceous materials,[153] some interesting results have been obtained by employing carbon nanotubes (CNTs),[154] that couple good electrochemical features with an extremely wide active area, assuring an efficient regeneration of the redox couple, especially if the latter is based on metal complexes. Yet, CNTs perform worst when a classical I-based electrolyte is employed; additionally, they are often produced by the exploitation of expensive and harsh templates.[155] This could make ineffective (from a sustainable point of view) their employment as deputy of platinum. Very recently, scientists started to exploit the use of organic waste materials as a carbon source to obtain Pt-free counter electrodes,[156–158] obtaining similar results compared to those of Pt-based devices. It should be pointed out, however, that the mere waste-derived origin is not enough to justify their employment; indeed, if the processes required to transform the carbon-based waste in a valuable cathode are expensive (e.g., high temperatures are used) or by-products (e.g., CO_2) are released during the process, the replacement of the platinum becomes pointless. Unfortunately, all carbonaceous materials sizeably suffer of instability toward the corrosive I-based electrolyte[151] that, notwithstanding the well-known and previously mentioned drawbacks, is the one actually employed in conventional and commercial DSSCs modules.

Due to the relative short stability assured by carbonaceous counter electrodes (at least in conventional devices), other classes of materials have been successfully investigated.[149] Among them, transition metals-based compounds are the materials of election because they couple remarkable catalytic activity (toward the most employed redox couples) and good charge transport properties with chemical, physical and (photo) electrochemical stability. Moreover, transition metals-based inorganic compounds are widely known to be very robust and cheap; additionally, they could be obtained as quasi-transparent thin films (transmittance values higher than 90% have been reported),[159–161] opening the door to the application in both indoor and BIPV. As a matter of fact, they could be considered as the best trade-off between PCE, stability, and environmental impact. The only concern related to this class of material lies in the choice of the metal to be employed. For example, the use of substances known as CRMs (e.g., chromium or cobalt) is not in line with large-scale production.

Sulfides,[162] especially the ones based on molybdenum,[163] iron,[164] copper,[165] titanium,[166] or nickel,[160] have been exploited due to low cost and easy synthesis: indeed, they could be obtained by chemical bath deposition,[163] atomic layer deposition,[167] hydrothermal approach,[168] and spin-coating of preformed NPs.[169] The tunability of synthetic approaches allow to obtain materials with tailored properties optimizing—simultaneously—morphological features and chemical bonding with the substrate. Studies on the long-term stability of S-based counter electrodes are not available, but it could be likely expected that they could undergo some unwanted reaction when in contact with metal-based redox couples (e.g., based on copper, cobalt or iron), due to the formation at the electrode/electrolyte interface of metallic sulfides. One strategy to avoid this is the replacement of sulfur with selenium, that it is chemically homologous.[170] Deposition approaches could be easily borrowed from sulfides ones,[171] but electrochemical methods have also been exploited.[172] The best results have been obtained with tin, vanadium and nickel selenides,[171–173] being the latter of particular interest also for the application in BIPV projects.

In DSSCs, transition metal oxides are usually employed as semiconductor electrode to be sensitized in order to harvest the largest portion of the solar radiation. Whereas n-type oxides (e.g., TiO_2) are employed as photoanodes in classical devices, p-type counterparts have been also exploited in inverted DSSCs.[174] The latter, being able to effectively collect and transfer holes (i.e., regenerate the oxidized species of the redox couple), could also be implemented as counter electrode in conventional devices. Compared to their Se- and S-based analogues, they are more robust, inert and easier to produce; on the other hand, they suffer for reduced surface area and morphological tunability. Copper is the element of election for this role, mainly due to its low cost and large availability:[175] indeed, both single,[176] double,[177] and ternary oxides[178] have been successfully tested.

As briefly discussed above, both the carbonaceous materials and the transition metals-based compounds present some advantages and drawbacks. To boost the former and minimize the latter, scientists effectively tested composite materials in which the electronic properties of carbonaceous materials are coupled with the robustness of inorganic sulfides and oxides. Usually, 2D scaffolds, such as graphene,[179,180] reduced graphene oxides (rGO),[181] or CNTs,[182] in which NPs are dispersed, are used. Albeit PCE values comparable or even better than those of Pt-based devices have been obtained with the use of composites, the latter are quite expensive and relatively hard to be recycled, jeopardizing their application at a large scale devices.[183,184]

A list of the principal keywords representing the state-of-art research in the field of DSSCs counter electrodes is shown in **Figure 3**.

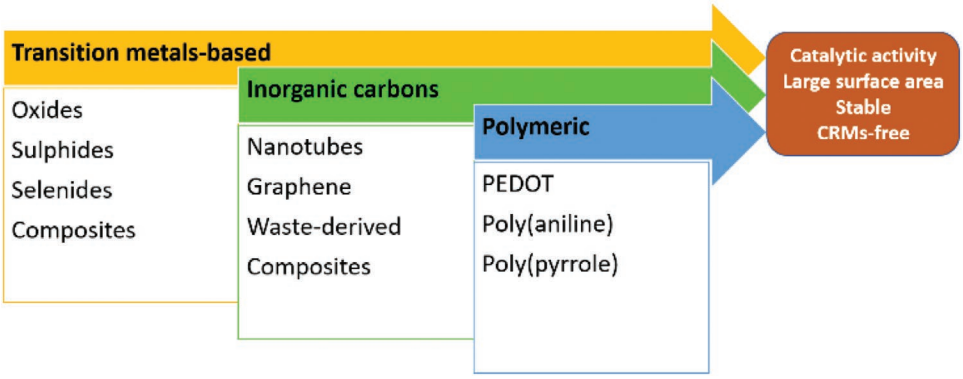

Figure 3. Main keywords of current research efforts in the development of counter electrodes for DSSCs.

In the following sections of this review, we will focus our attention on the implementation of a specific class of polymeric materials, based on PEDOT, as both counter electrode (Section 3) or solid-state conductor (Section 4) in DSSCs.

3. Poly(3,4-ethylenedioxythiophene) and Poly(3,4-ethylenedioxythiophene)-Based Systems for Dye-Sensitized Solar Cells Counter Electrodes

As described in the previous section, the most used counter electrode for DSSCs is platinum: a nanometric film of this metal can be deposited on F-doped SnO_2 (FTO) by means of different techniques, such as sputtering or thermal decomposition of H_2PtCl_6.[185,186] Despite its high work function and strong catalytic activity, the main problems associated with the use of Pt are given by its scarcity, high-temperature deposition and corrosion by I-based redox couple.[187] The latter leads to the formation of soluble PtI_4^-, thus reducing the number of iodide ions addressed to the regeneration of the oxidized dye molecules.[188] Therefore, the replacement of Pt-based cathodes is necessary for the large-scale fabrication of DSSCs.

PEDOT could be a suitable alternative to platinum, due to its low cost, ease of deposition, high transparency and suitable potential. In this section, the main application of PEDOT and PEDOT-based material as counter electrodes in the DSSCs field are reviewed.

3.1. Pure Poly(3,4-ethylenedioxythiophene)

One of the first examples of the use of pure PEDOT as cathode for DSSCs was reported by Pringle et al. in 2009.[189] It led to remarkable PCE values in cells assembled with both acetonitrile- and ionic liquids-based electrolytes, that is, 7.82% and 4.78%, respectively, performance comparable to those provided by Pt-based devices, that is, 7.90% and 5.06%, respectively. The good behavior of PEDOT as counter electrode material was also confirmed in the presence of gel electrolytes,[190] even if with PCE values slightly lower (6.4%) due to slower charge transfer in the quasi-solid state electrolyte.

In the following years, many synthetic strategies were explored, such as chemical synthesis,[191] electropolymerization,[192–196] solid state polymerization,[197] and oxidative molecular layer deposition.[198] In particular, the role of polymerization time, precursor concentration, substrates and templating agents was explored. Electrochemical synthesis is a low-cost and low energy demanding technique, that allows the deposition of a thin film on a conductive solid substrate. It is more effective and rapid with respect to traditional chemical route. In addition, it allows a strict control over the film morphology.

Pringle et al. were the first authors reporting the electrodeposition of PEDOT onto conducting flexible substrates, that is, poly(ethylene naphthalate) (PEN) made conductive with In-doped SnO_2 (ITO), demonstrating that this strategy was also valid for industrial scale roll-to-roll technique.[192] The effect of deposition time (ranging from 5 to 45 s) was investigated. A deposition time of 5 s generated a compact and dense PEDOT film, as confirmed by scanning electron microscopy (SEM) analysis (**Figure 4**A). When the deposition time was increased to 45 s, the surface became granular and rough. PEDOT/ITO-PEN cathodes reached comparable PCE values to those provided by Pt/FTO: 8.0% versus 7.9%, 5.0% versus 4.8%, and 5.7% versus 5.6% in electrolytes formulated with acetonitrile, $[C_2mim][SCN]$, and $[C_2mim][B(CN)_4]$ solvents, respectively.

The effect of the polymerization time was also explored by Ahmad and coworkers.[193] The electrochemical synthesis was performed on FTO immersed in ionic liquid, where EDOT precursor was dissolved. The polymerization time was explored between 30 and 120 s. However, in this case, no evident influence of the reaction time was observed: as a matter of fact, in both cases a homogeneous morphology with porous structure was observed. The PCE values ranged from 7.86% to 7.93%, in accordance to what reported by Pringle et al.[192]

Xiao et al. reported three different electrochemical techniques for the synthesis of PEDOT onto FTO glass:[194] Cyclic voltammetry (CV), constant potential and constant potential pulse. The layer surface of the sample obtained by CV was flaky and nonuniform, whereas the other two strategies led to uniform morphologies. PEDOT electrodes synthesized by constant potential pulse exhibited also the higher redox activity, the lowest charge-transfer resistance (R_{ct}, 1.27 vs 1.56 Ω cm^2 of Pt) and the highest PCE (6.40%).

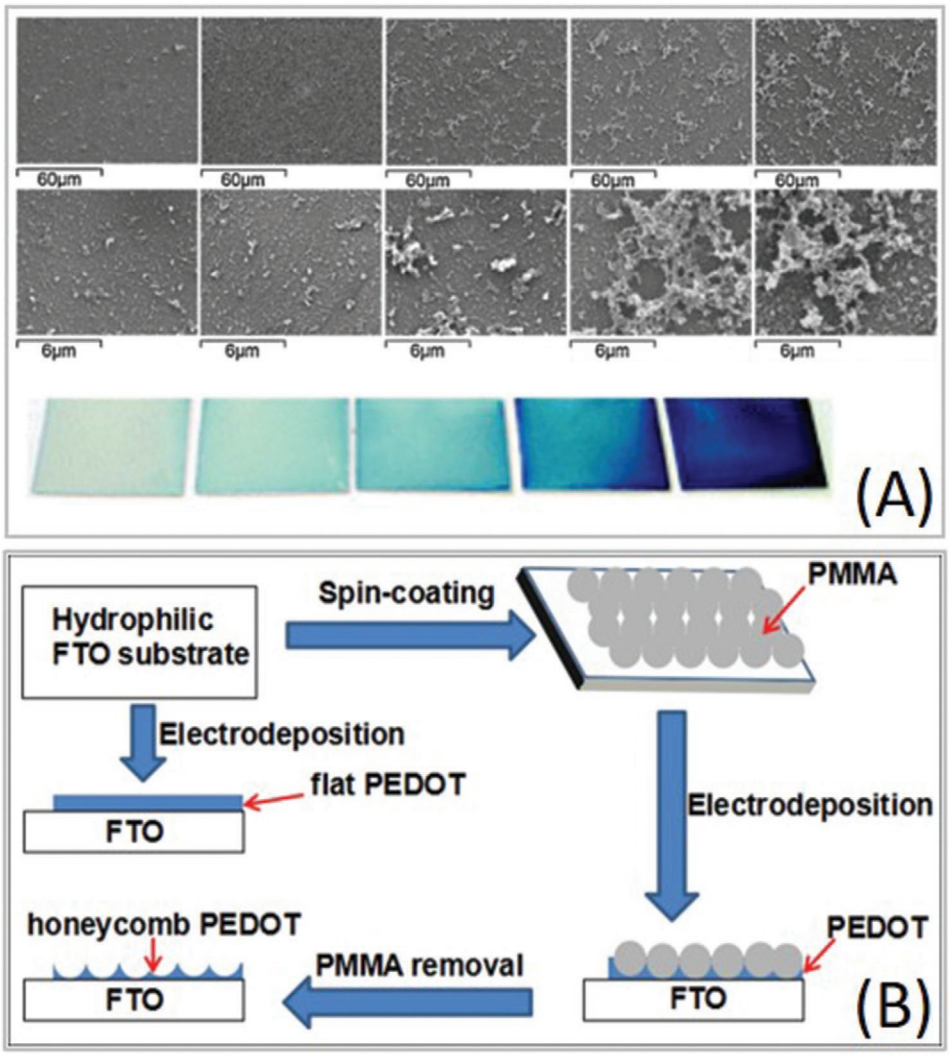

Figure 4. A) SEM images of PEDOT films on ITO-PEN, grown for (left to right) 5, 10, 15, 30, and 45 s; the corresponding digital pictures of the electrodes are shown below. B) Schematic illustration of honeycomb PEDOT fabrication, by using PMMA as sacrificial templating agent. Reproduced with permission.[192,205] Copyright 2010, RSC. Copyright 2017, Elsevier.

A further upgrade to the electrochemical technique is the use of low environmental impact solvents. As a matter of fact, ionic liquid or volatile organic solvents are often used for the preparation of PEDOT. As a better solution, water can be potentially used, as reported by Gao et al.[195] and Ellis et al.[199] According to what previously reported,[192] the porosity of the surface increased with the polymerization time. The PV parameters found for PEDOT-based devices were even better than those of Pt-based counterparts: 0.68 V, 16.66 mA cm^{-2}, 0.57 (fill factor, FF) and 6.46% with PEDOT-40 s, versus 0.68 V, 15.27 mA cm^{-2}, 0.61 and 6.33% with Pt.[195] Ellis et al. got a homogeneous PEDOT films on both FTO and flexible plastic substrates,[199] as shown in **Figure 5**A,B. Electrochemical impedance spectroscopy (EIS) measurements showed that the R_{ct} increased with the thickness of the layer; however, all measured R_{ct} values were smaller than those of Pt-based cathodes. The best PCE recorded in this work was 6.2%.

Solid-state polymerization represents an alternative, less scalable fabrication technique. In 2013, Yin et al. developed a spin-coating deposition for the precursor 2,5-dibromo-3,4-ethylenedioxythiophene precursor on both FTO and ITO-PEN substrates.[197] The deposition was followed by a low temperature annealing (80 °C), allowing the formation of solid PEDOT. The corresponding cell produced a PCE of 7.04%. Later, the influence of the annealing temperature was studied as well.[200] At the lowest temperature (40 °C), the resulting polymer presented a porous structure, with small NPs (50–80 nm diameter). A more uniform morphology was obtained by increasing the temperature till 80 °C. In addition, the film was thinner and showed a better adhesion on FTO. However, the best PCE reached by Chen et al. was 4.9%,[200] lower than that previously reported.[197]

In an interesting paper, Kim et al. used the oxidative molecular layer deposition to form a PEDOT film on an ITO substrate.[198] As clearly sketched in Figure 5C, the EDOT precursor

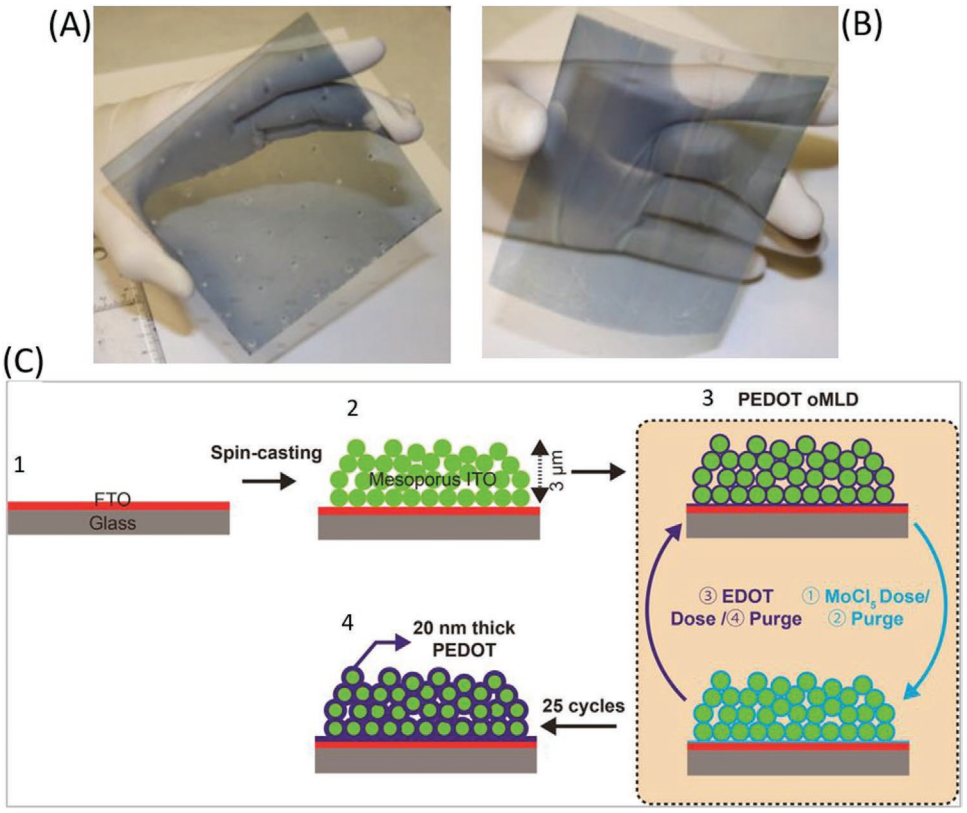

Figure 5. Photographs of PEDOT (obtained by aqueous micellar electrodeposition) onto A) FTO-glass and B) flexible ITO-PET substrates. C) Scheme for the preparation of PEDOT-coated mesoporous ITO films for a cathode in DSSCs using oxidative molecular layer deposition: 1) Cleaned FTO glass, 2) spun-cast ≈3 µm-thick mesoporous ITO onto FTO glass, c) PEDOT deposition, d) ≈20 nm-thick PEDOT film after 25 cycles of deposition. Reproduced with permission.[199,198] Copyright 2013, Elsevier. Copyright 2015, ACS.

was deposited on the surface of mesoporous ITO spheres and then treated with the oxidizing agent $MoCl_6$. Characterization revealed that the cathode material possessed high surface area and improved electron transport properties; a PCE of 7.18% was achieved. In an analogous way, the influence of PEDOT amount onto FTO glass was explored,[201] by using different EDOT precursor concentrations. The best performing device outperformed the one assembled with platinum (6.73%), reaching a PCE of 7.32%. Moreover, this cathode demonstrated a lower R_{ct} (1.00 Ω) with respect to that of Pt (2.55 Ω).

The effect of PEDOT nanostructure was investigated by Trevisan et al.[202] Since the counter electrode is involved in an electrocatalytic reaction, the surface area must be optimized. The author tested two PEDOT morphologies, that is, flat and nanostructured arrays, using the electropolymerization method in both cases. The two devices were filled with an I-based electrolyte, containing a mixture of acetonitrile and valeronitrile as solvent. As expected, the nanostructured cathode slightly outperformed the flat one (8.3% vs 7.9%). The PV performances of the nanostructured PEDOT were strongly influenced by the electrolyte: as a matter of facts, the PCE decreased to 6.3% when methoxypropionitrile was used as electrolyte solvent. This drop was due to both a decrease of V_{oc} (from 0.72 to 0.68 V) and J_{sc} (from 16.24 to 13.13 mA cm^{-2}). The latter electrolyte exhibited also a higher R_{ct} from EIS study.

Another fundamental aspect to be considered is the efficiency in transporting charges from the FTO to the electrolyte. In this sense, a 1D nanostructure could be more effective with respect to the bulk material or 0D NPs. Lee et al. reported a PEDOT nanofiber (NF)-based counter electrode obtained in water by using sodium dodecyl sulfate and $FeCl_3$ as surfactant and initiator, respectively.[203] The resulting material had a porous channels structure, which could facilitate the penetration of the liquid electrolyte. In addition, the electron transfer from the FTO to the electrolyte was faster with respect to what observed for the bulk material, because of a reduction of grain boundaries and internal resistance. Consequently, the PCE of the PEDOT:NF-based device (9.2%) was far above that of the bulk PEDOT-based one (6.8%) and outperformed also the state-of-art Pt-based system (8.6%).

In general, in a liquid or gel-polymer electrolyte both anions and cations move within the two electrodes. This phenomenon causes a polarization of the electrolyte media, with an increase of the internal resistance. On the other hand, polymeric ionic liquids (PILs) are single-ion conductors in which anions or cations are chemically bonded to the polymer backbone, therefore reducing the internal resistance. Jeon et al. used a PIL as electrolyte and coupled it with a PEDOT:NF cathode.[204] Different amounts of the single-ion conductor poly(1-methyl-3-(2-acrylic oxypropyl) imidazolium iodide (PMAPII) were introduced into the liquid electrolyte. A remarkable PCE of 8.12% was reached,

when PMAPII content was 16 wt%, whereas Pt-based device showed a PCE of 6.85% under the same conditions. The PCE was comparable to that of the fully liquid cell (8.34%).

Another kind of morphology was investigated by Li et al.[205] A PEDOT cathode with honeycomb-like morphology was synthesized by using poly(methyl methacrylate) (PMMA) mould as templating agent (Figure 4B). Three different amounts of PMMA were used: h-PEDOT-1 (6 wt% PMMA), h-PEDOT-2 (8 wt% PMMA), h-PEDOT-3 (10 wt% PMMA). For comparison also flat PEDOT was tested (f-PEDOT). Field emission SEM (FESEM) images showed that h-PEDOT-2/PMMA had a diameter of 150–200 nm and a thickness of 150 nm. After depositing PEDOT and removing PMMA-2, the remaining thickness was 80 nm, with honeycomb-like morphology and high surface area. CV measurements showed that the order of cathode current densities was as follows: h-PEDOT-2 > h-PEDOT-3 > h-PEDOT-1 > f-PEDOT. Thus, the h-PEDOT-2 conformation was the most electrochemically active. EIS measurements also confirmed that the sample with the lowest internal resistance was the h-PEDOT-2. The results obtained from PV characterization of DSSCs assembled with for h-PEDOT-2 were: J_{sc} = 17.72 mA cm^{-2}, V_{oc} = 768 mV, FF = 0.67, and PCE = 9.12%, and were the highest ever among all the different types of counter electrodes tested and mentioned in the article.

The effect of the substrates was investigated as well. In the different papers described below, PEDOT polymer was deposited on carbon,[206] antimony-doped SnO_2 (ATO),[207] and Pt.[208]

Thompson et al. deposited PEDOT by electropolymerization on C-based cathodes in a monolithic DSSC.[206] The advantage of this architecture is the halved need for expensive FTO glass. SEM images confirmed that the polymer forms an interconnect network within carbon particles. Therefore, additional conductive pathways and particles adhesion were provided. As a matter of fact, the presence of PEDOT decreased the series resistance (R_s) from 52 to 12 Ω cm^{-2} and the FF of the corresponding devices was improved from 0.29 to 0.67. Finally, the PCE was almost doubled passing from the PEDOT-free device (2.3%) to the PEDOT-based one (5.2%).

In the work by Xia et al., PEDOT was deposited on ATO NPs.[207] The ATO layer was porous and the average NPs dimension was 20 nm. This high surface area structure was retained after the polymerization of EDOT, as reported by SEM images. The CV analysis demonstrated the high electrocatalytic activity and reversibility of PEDOT/ATO with respect to Pt and bare ATO and PEDOT; in fact, the ratio between the anodic and the cathodic current peak reached the lowest value for PEDOT/ATO. The PCE values of the corresponding devices were 7.54, 7.47, 6.09, and 2.07% for Pt, PEDOT/ATO, PEDOT, and ATO, respectively.

In a similar way, Ma et al. used Pt NPs anchored on the surface of ITO-PEN, and then added a thin layer of porous PEDOT.[208] SEM characterization further confirmed the interconnected assembly between Pt and PEDOT, with positive consequence on charge transport.

3.2. Poly(styrene sulfonic acid)-Doped Poly(3,4-ethylenedioxythiophene)

Pure PEDOT is supposed to work as HTM. When doped with anions, such as PSS, it can work also as electrons carrier, thus improving its efficiency as cathodic material in DSSCs. In this section, the used of anion-doped PEDOT counter electrodes is reviewed.

One of the first examples of PEDOT:PSS used as counter electrode for DSSCs was reported by Balraju et al., with a poor PCE of 4.10%.[209] Similar PCE were obtained also with polymer electrolytes based on poly(ethylene oxide) (PEO, 4.08%) and poly(ethylene glycol) (PEG, 3.87%).[210] However, when PMMA and poly(vinyl acetate) were used in the electrolytes, a drop of PCE was observed (PCE < 1%). In fact, when the latter polymers were used, the R_{ct} at the cathode/polymer electrolyte interface was really high, as confirmed by EIS studies. The PMMA-based electrolyte was also studied by Biancardo et al.;[211] the electrocatalytic activity of the PEDOT:PSS was appropriate, but PCE values were still low, ranging from 0.20 to 0.37%.

Despite its demonstrated working activity, the main drawbacks when using PEDOT:PSS as counter electrode material is still its low conductivity (commonly measured as ≤ 1 S cm^{-1}), due to the disordered PSS chains within the PEDOT matrix. Anyway, the conductivity of PEDOT:PSS can be enhanced by three orders magnitude, by following several routes, such as thermal treatments,[212,214] acid treatment,[215] solvent treatment,[216] or by increasing the molecular weight. Otherwise, PCE values remain low, since the conductivity—even if improved—is still low. The impact (on costs and environment) of each of these processes has not been addressed in the literature, even if use of solvents and high temperature steps must be carefully evaluated and correlated with the resulting cell stability and PCE.

Park et al. first explored the effect of temperature on the morphology and electrocatalytic properties of PEDOT:PSS.[212] The annealing temperature ranged between 45 and 60 °C and the thermal treatment lasted 20 min. However, no evident effect was observed in terms of PCE (2.48–2.49%). Only when the thermal treatment was extended up to 720 min cells with PEDOT:PSS treated at 45 °C gave the best PCE of 3.22%. However, the increase of the thermal treatment time has a negative effect, considering the sustainability of the whole fabrication process, due the increased energy demand. SEM characterization revealed that, at that temperature, the surface had a granular structure that, potentially, increased the surface area and the number of active sites. Similar results have been obtained also by Shenouda et al.[213] Chou et al. further investigated the effect of the annealing duration and temperature.[214] Authors treated the PEDOS:PSS thin layer at 80, 100, and 120 °C for 0–15 min. It was found out that, at a fixed annealing temperature, increasing the duration of the thermal treatment made the morphology of the PEDOT:PSS film evolve from drop-like particles, randomly dispersed on the FTO glass, into earthworm-like bars, homogenously dispersed in the film. Therefore, the longer annealing time facilitated the cross-linking of well-conducting PEDOT moieties in the less conducting PSS matrix. As a matter of fact, the best PCE (6.37%) was reach for the PEDOT:PSS treated at 120 °C for 15 min.

The main drawbacks of the thermal treatment are high energy demand, poor safety, and reproducibility. Yeon et al. obtained a high conductive PEDOT:PSS polymer by using a HNO_3 treatment at room temperature;[215] anyway, the potential

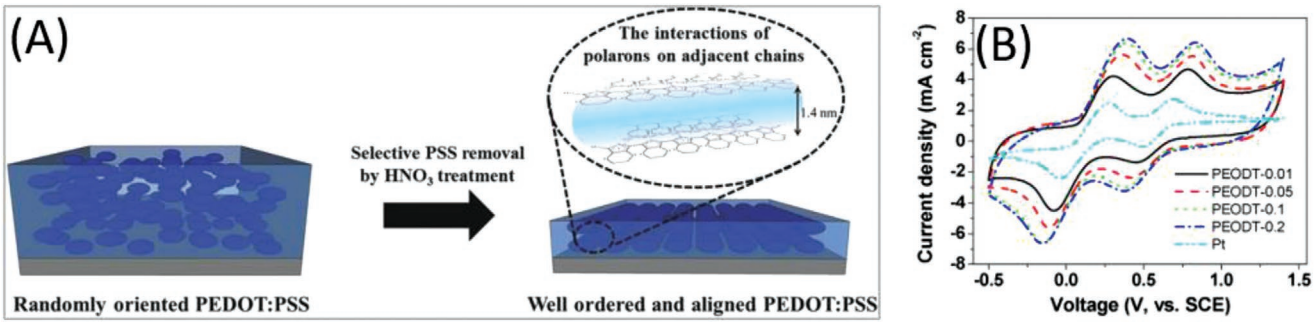

Figure 6. A) Scheme of the structural rearrangement of the PEDOT:PSS film after the HNO_3 treatment, where it is highlighted that the amorphous PEDOT:PSS grains are rearranged to a crystalline PEDOT:PSS structure through the selective removal of PSS by HNO_3. B) CV curves of I^-/I_3^- redox couple with PEDOT- and Pt-based electrodes (scan rate: 50 mV s^{-1}; electrolyte: LiI 10 mM, I_2 1 mM, and $LiClO_4$ 0.1 M in acetonitrile). Reproduced with permission.[215,224] Copyright 2015, Wiley-VCH. Copyright 2015, Elsevier.

release of NO_x was not assessed in the study. The conductivity of HNO_3-treated PEDOT:PSS was remarkably high (4100 S cm^{-1}), with respect to the pristine or thermal treated-ones. The effect of the acid treatment was the enlargement of the interlayer distance between PEDOT and PSS, as reported in **Figure 6**A; in fact, the strong coulombic attraction between positively-charged PEDOT and negatively-charged PSS can be shielded by the ionic species present in HNO_3. The PEDOT-rich chains aligned along a preferred orientation and this resulted in a low energy barrier for the charge transport process. The conductivity enhancement was due to an improvement of both the carrier concentration and their mobility. The best PCE reached in this work was 8.61%.

Another way to improve conductivity is solvent-treatment. This strategy is relatively simple and reproducible. In 2013, Chiang et al. reported a counter electrode composed by PEDOT:PSS deposited onto a poly(ethylene terephthalate) (PET) substrate, thus avoiding the use of both Pt and FTO.[216] A solvent-treatment of PEDOT:PSS was performed with ethylene glycol and hexafluoroisopropyl alcohol. The latter possesses a hydrophobic $-CF_3$ group that preferably interacts with the PEDOT chain, whereas the hydrophilic alcoholic hydroxy group effectively interacts with PSS. The phase segregation and ordered orientation between PEDOT and PSS was thus facilitated. In addition, the solvent-treated PEDOT:PSS had denser morphology, as demonstrated by X-ray diffraction (XRD) and atomic force microscopy (AFM) studies. Moreover, the sheet resistance of the solvent-treated PEDOT:PSS ranged from 1.30 to 6.84 Ω sq^{-1}, depending on the amount of solvents used (more solvent led to lower resistance values, but to a more impactful process). The sheet resistance of the pristine commercial PEDOT:PSS was five order magnitude higher (40 264 Ω sq^{-1}). The PEDOT:PSS-based device demonstrated a PCE of 7.29%, which was close to that of the traditional Pt/FTO one (7.62%).

Liu et al. exploited PET-based flexible substrates for DSSCs as well.[217] PEDOT:PSS could be a suitable material because it does not require high temperature annealing. Therefore, its use allows i) the use of flexible substrates and ii) the use of the scalable roll-to-roll technique. PEDOT:PSS was deposited on PET substrate by roll-to-roll slot-die coating. To further increase the conductivity, an additional layer of PEDOT was deposited on the top of the PEDOT:PSS layer by electropolymerization. PEDOT:PSS/PET exhibited a flat surface, that did not offer enough reaction centres. On the other hand, the addition of an electropolymerized PEDOT layer increased the roughness and the surface area. The amelioration of the redox properties of the cathode was also confirmed by *J–V* measurements. The PCE values were 0.93 and 4.84% for PEDOT and electropolymerized PEDOT based cells, respectively.

3.3. Anion Doped-Poly(3,4-ethylenedioxythiophene)

Xia et al. tested the effect of using different supporting electrolytes during the electrodeposition of PEDOT films on FTO glass.[218] Therefore, three different kind of materials were obtained, namely PEDOT-ClO_4, PEDOT:PSS and PEDOT-TsO (when ClO_4^-, PSS^-, and TsO^- were used as counter ions, respectively). SEM images revealed a homogeneous morphology in all these cases. The Pt-based cell reached the highest PCE of 4.3% (a good value in 2007), not so different from that achieved by the PEDOT-based devices (4.0–4.2%). This demonstrated that the counter ions had relatively low influence on PCE values, as long as an appropriate catalytic efficiency was provided.

Saito et al. investigated the difference between PEDOT:PSS and PEDOT:TsO as well.[219] The CV was used to investigate the electrocatalytic properties of bare glass, platinum, PEDOT:TsO, and PEDOT:PSS. In the case of bare glass, the redox reaction was absent and there were no peaks in the curve. With PEDOT-PSS, the oxidation current was lower with respect that of the Pt-based substrate. An explanation may be the reduction of the active sites of PEDOT, since PSS could preclude the access of the electrolyte to the PEDOT chain. Instead, the PEDOT-TsO promoted a regular exchange with the electrolyte. Consequently, PEDOT:TsO device exhibited a PCE (4.60%) double with respect to that of PEDOT:PSS-based counterpart (2.10%) and really close to that of Pt-based cell (4.67%). The same authors further evaluated the influence of PEDOT:TsO film thickness.[220] CV measurements showed that the current density increased with the PEDOT thickness. The R_{ct} decreased with the PEDOT thickness; in fact, an increase of the thickness resulted in an improvement of the surface area and, therefore, of the number of catalytic centers. Thus, the best PCE of 3.6% was reached with the highest PEDOT thickness (i.e., 2 μm).

A way to improve the performance of PEDOT:TsO is the enlargement of pore size, that causes the creation of a larger

number of active sites.[221] The pristine PEDOT:TsO forms an homogeneous film, with an average pore size of 10–20 nm. The latter can be enhanced by the chemical treatment with hydrazine and iodine. It was demonstrated that, after a reduction treatment with hydrazine, the pore size increased to 200–300 nm. A subsequent oxidation treatment using iodine vapor further increased the pore size up to 300–500 nm, confirming that the treatments influenced the porosity. From the sustainability point of view, this high temperature treatment with corrosive I_2 has surely a negative impact. The PEDOT:TsO treated with both hydrazine and I_2 reached a remarkable PCE of 6.86%, while the pristine material had a PCE = 4.93%. In particular, the FF shifted from 0.48 to 0.64, evidencing the more proper operation of the cell with reduced sheet resistance and the better interface with the electrolyte.

Jiang et al. prepared a PEDOT:ClO_4 counter electrode by means of a facile electrochemical deposition method, by using EDOT and $LiClO_4$ in acetonitrile as precursor and supporting electrolyte, respectively.[222] However, the obtained PCE was quite low (0.88%). To further improve charge transfer at the cathode and, therefore, the overall PCE, a layer of TiO_2 was deposited on PEDOT:ClO_4. The TiO_2 deposition time was ranged between 5 and 35 s. EIS measurements showed that the R_{ct} decreased with the TiO_2 deposition time to a minimum of 2.12 Ω cm^2. The best PCE (1.23%) was obtained by a deposition duration of 25 s. To further increase this modest performance, the use of reflective light may be effective:[223] a suitable way to exploit the reflective light is to put a reflective material, such as TiO_2, on the cathodic side of the cell. The same authors reported the deposition of both TiO_2 particles and TiO_2 thin film onto TCO glass by sol–gel technique. Then, a film of PEDOT:ClO_4 was deposited by electropolymerization to fabricate the counter electrode. In this way, the PCE was improved from 3.85% (pristine PEDOT:ClO_4) to 4.61% (TiO_2 particles/PEDOT:ClO_4) and 4.55% (TiO_2 thin layer/PEDOT:ClO_4).

Han et al. investigated the influence of EDOT monomer concentration on the performance of the counter electrode consisting of PEDOT:ClO_4 electropolymerized in situ.[224] The influence of monomer concentration is reflected on growth, morphology, conductivity, and catalytic activity. SEM images showed that PEDOT generally exhibited a porous surface, but by increasing the monomer concentration from 0.01 to 0.2 M the morphology was flatter and the thickness increased: 1.55, 2.46, 2.66, and 2.73 μm for PEDOT-0.01, PEDOT-0.05, PEDOT-0.1, and PEDOT-0.2 (where the number indicates the molar concentration of EDOT). By increasing the amount of monomer, it was observed that the conductivity decreased. It is well known that the conductivity of an organic polymer is correlated with the doping level, therefore—with the same amount of $LiClO_4$—PEDOT derived from a lower initial EDOT concentration showed the highest conductivity; resistivity tests confirmed this thesis. CV measurements (Figure 6B) were carried out and it was observed that the peak-to-peak separation increased when raising the EDOT concentration, so PEDOT obtained from lower EDOT concentration values showed better electrocatalytic activity. EIS measurements showed that R_{ct} increased with higher EDOT concentration values from 2.9 Ω (PEDOT-0.01) to 5.9 Ω (PEDOT-0.2), so PEDOT derived from a lower EDOT concentration had a better charge transfer rate. PV performance confirmed that the best cathode was the one cured with EDOT 0.05 M, that showed V_{oc} = 0.731 V, J_{sc} = 14.18 mA cm^{-2}, FF = 0.68, and PCE = 7.42%.

3.4. Modified Poly(3,4-ethylenedioxythiophene)

Despite many PEDOT-based devices reported in the literature are assembled using liquid electrolytes, solid polymer electrolytes have also been reported. Most of these solid systems are based on PEO or its derivatives. They ensure better long-term stability with respect to liquid counterparts, even if their use results in high interfacial resistance. To improve the interfacial contact between the solid electrolyte and the and cathode, chemical compatibility must be provided. For this reason, Kim et al. reported PEDOT-g-PEG as cathodic material for DSSCs.[225] The polymer was casted onto FTO to fabricate all-solid-state DSSCs, employing a PEO-based solid electrolyte. The modified PEDOT counter electrode led to high transparency, remarkable interfacial properties with the electrolyte, and good electrocatalytic behavior. As a matter of fact, the PCE was 8.45%, comparable to that of Pt (8.25%) and higher that than of PEDOT (7.83%).

Metal-ion doping is a possible strategy to improve the catalytic activity of PEDOT. Wu et al. studied the effect of metal-ion doping (Mn^{2+}, Co^{2+}, Ni^{2+}, and Cu^{2+}) on PEDOT deposited on ITO-PEN substrates.[226] SEM images showed that pure PEDOT was irregularly sized, comprising stacked particles with no channels for charge transfer. PEDOT-Co^{2+} and PEDOT-Ni^{2+} presented an interconnected structure between the particles. PEDOT-Cu^{2+} and PEDOT-Mn^{2+} featured particles of various sizes (from 100 nm to 2.0 μm) with channels that also increased porosity and surface area. PEDOT-Mn^{2+} led to the best performance (PCE = 5.19%). Finally, CV, EIS, and Tafel polarization tests were conducted to confirm the superiority of PEDOT-Mn^{2+} and confirmed the trend of V_{oc} and J_{sc} values. In general, in all tests the trend of the obtained values (cathodic current density, peak-to-peak separation, R_{ct} and exchange current density) followed this order: PEDOT-Mn^{2+} > PEDOT-Ni^{2+} > PEDOT-Co^{2+} > PEDOT-Cu^{2+}, confirming that PEDOT-Mn^{2+} possessed the best activity and reversibility. Nevertheless, the use of rare metals, such as cobalt, is controversial.

If solid-state electrolytes represent a good solution for stable DSSCs (even if some issues remain, as already described in previous sections), another promising challenge regards the use of water-based electrolytes. This would ensure a better DSSC technology in terms of sustainability, safety, and end-of-life disposal.[125,126] PEDOT-based cathodes were explored also in this emerging field, addressing one of the issues regarding the use of PSS: it shows electrostatic repulsion between negatively with I_3^-, that is, the ions that have to be reduced at the cathode. To overcome these issues, Bella et al. proposed a modified PEDOT with a cationic ammonium moiety and iodide as counterion, namely cPEDOT.[227] Since this polymer is water-soluble, it was mixed with (3-glycidyloxypropyl)trimethoxysilane to avoid any possible detachment from the FTO-glass electrode when an aqueous electrolyte was used. The mixture was deposited by spin coating; a subsequent thermal treatment resulted in the crosslinking of the FTO/silane/cPEDOT. The electrode showed remarkable cathodic current and small potential difference

between anodic and cathodic peaks, highlighting its good catalytic properties. In addition, cPEDOT afforded a R_{ct} (3.29 Ω) lower with respect to that of platinum (5.33 Ω). It was used to fabricate aqueous DSSCs and remarkable PV parameters were obtained (0.69 V, 12.41 mA cm^{-2}, 0.77, 6.64%), also being better than those obtained with PEDOT:PSS (0.65 V, 8.88 mA cm^{-2}, 0.61, 3.53%) and platinum (0.66 V, 11.05 mA cm^{-2}, 0.68, 4.95%).

3.5. Poly(3,4-ethylenedioxythiophene) Laden with Carbon-Based Materials

3.5.1. Graphite/Carbon

PEDOT and PEDOT:PSS are interesting and efficient counter electrode materials, due to their demonstrated electrocatalytic activity; however, the overall low conductivity may impede a fully successful use in DSSCs. The hybridization with C-based materials could be a suitable strategy for improving conductivity and efficiency of redox shuttle regeneration, even if the sustainability aspects of this approach must be evaluated as well. In a perspective of circular economy and environmental friendliness, the use of waste-derived carbon and low impact processes is preferable; some literature works are present with these aims, but a LCA study has never been provided.

A PEDOT:PSS/graphite/carbon black composite material was successfully created by Yue et al.[228] The CV measurements in I- and acetonitrile-based liquid electrolytes demonstrated higher current density peaks (for both oxidation and reduction processes) than those of state-of-art Pt-based electrodes. These results highlighted that PEDOT:PSS/C could lead to lower resistance and higher conductivity values, thus being a suitable replacement for platinum. The *J*–*V* measurements showed that the cathode composed by PEDOT:PSS/C led to PV performances closer to those achieved in the presence of platinum (7.01 and 7.78%, respectively).

Other studies were carried on by the same group.[229] In particular, authors exploited PEDOT:PSS/C composites as cathodic materials for all-solid-state DSSCs. The cell architecture is reported in **Figure 7**A and different annealing protocols were adopted; the first type of cell was annealed under vacuum at 80 °C, the second one in air at 80 °C. The *J*–*V* curves showed that PEDOT:PSS/C led to better performance than those obtained with Pt-based counterparts, with PCE of 4.11% and 3.42% for the vacuum- and air-treated cells, respectively. The influence of the annealing conditions and temperature was further investigated in a following paper.[230] Despite what already reported, it was observed that the annealing conditions had minimal influence on the conductivity and sheet resistance of the PEDOT:PSS/graphite composite, that assumed the values 1.73 S cm^{-1}, 11.94 Ω sq^{-1}, 1.72 S cm^{-1}, and 11.94 Ω sq^{-1} for the vacuum- and air-treated electrodes, respectively. Finally, PV performances were studied for different annealing temperatures (40, 60, 80, 100, 120, and 140 °C), obtaining the best performance always at 80 °C for both series.

Wang et al. reported the deposition of PEDOT on carbon nanospheres.[231] The carbon layer was obtained by the deposition of a C-based ink, whereas PEDOT was electropolymerized on carbon. In their paper, for the first time the authors used

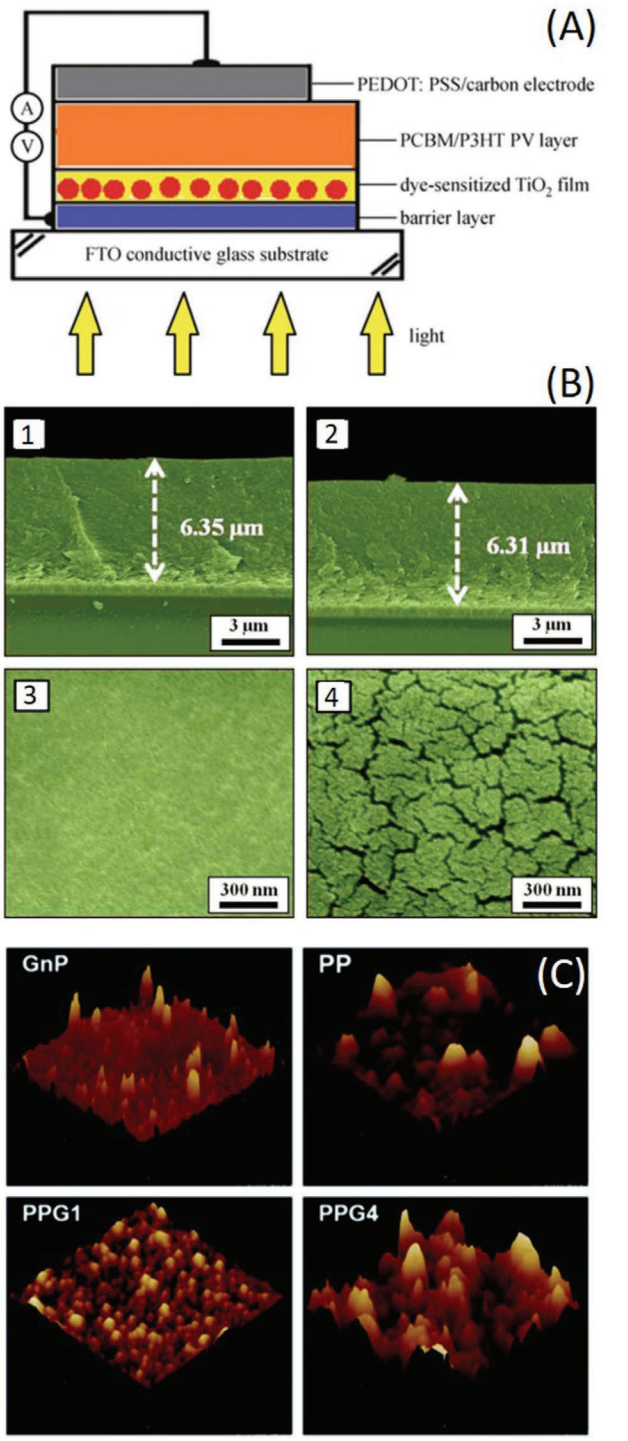

Figure 7. A) Scheme of TiO_2/dye/PCBM/P3HT/PEDOT:PSS/C solar cell. B) Cross sectional images of 1) PEDOT:PSS and 2) PEDOT:PSS/GDs films, along with their 3,4) corresponding top view images. C) AFM images of GNPs, PEDOT:PSS (indicated as PP) and PEDOT:PSS/GNPs composites onto FTO glass. Reproduced with permission.[229,242,245] Copyright 2011, Springer. Copyright 2015, Elsevier. Copyright 2018, RSC.

PEDOT in combination with S-based ionic liquid electrolytes. It was demonstrated the ability of PEDOT/C composite to effectively reduce the redox couple and therefore acting as proper

cathodic material. The optimized PCE was 6.5%, while the stability was not assessed.

Nagarajan et al. employed exfoliation as a strategy to boost the catalytic activity of graphite-based materials, testing for the first time a PEDOT/EFG (EFG = exfoliated graphite) as cathode for DSSCs.[232] High resolution transmission electron microscopy (TEM) showed that EFG sheets were crystalline with internal cracks, but when PEDOT was inserted the composite became flexible without showing cracks. The flexibility was attributed to the fibres of PEDOT that reinforced the surface, giving it more elasticity. SEM images showed that the cathode possessed a high surface area and a highly porous structure, indicating good catalytic activity. EIS confirmed that the internal cell resistance decreased dramatically passing from pristine EFG to PEDOT/EFG, as also underlined by the increase of FF values. The PCE of PEDOT/EFG-based cells reached a value of 5.78%, that was even higher than that of the corresponding Pt-based cell. A better exfoliation was implemented by Belekoukia et al., where graphite was exfoliated by electrochemical method at 10 V.[233] This technique presented several advantages; indeed, the such obtained graphene possessed large lateral size, good charge transport properties, and low oxidation degree. In addition, the synthesis was carried out in distilled water at room temperature and was very rapid (10 min). The use of dimethylformamide in the purification step was the main drawback of this technique from the sustainability viewpoint. As a matter of facts, the corresponding device reached a PCE value of 8.0%.

Within the circular economy framework, the use of renewable materials is a fundamental aspect.[20] The exploitation of bio- and waste-derived carbon materials is extensively studied. Nonetheless, the carbonization of these matrices usually requires high temperature and inert atmosphere, threating the sustainability of the entire process. As an example, Moolsarn et al. investigated a PEDOT/C composite, where the C-based material was obtained by the carbonization of human hair.[234] The composition of the latter was first studied: amino acid, keratin, melanin, and protein. All these molecules are composed of carbon, oxygen, nitrogen, hydrogen, and sulfur. Through XRD patterns, it was observed that—after carbonization at 700 °C—some nitrogen, oxygen, and sulfur residues remained, so the temperature was not high enough to expel all heteroatoms. Both EIS and CV measurements showed good catalytic activity (through cathodic current density and R_{ct} measurements), even if that of Pt was still better. Under the best conditions, the following PV parameters were obtained: V_{oc} = 0.76 V, J_{sc} 14.85 mA cm^{-2}, FF = 0.58, and PCE = 6.54%.

3.5.2. Graphene

Graphene is a promising 2D material, composed by planar covalently bounded carbon atoms. It demonstrates remarkable catalytic and electronic properties, due to the delocalized p electrons. In addition, its transparency makes it even more attractive for optoelectronic applications.[235–237]

The functionalization of graphene resulted in modified electronic and optical features or self-assembly properties. For example, the non-covalent functionalization with 1-pyrenebutyrate is useful for dispersing it in aqueous solution.[238] Graphene can be mixed with PEDOT:PSS and spin coated on ITO substrates. In this way, a transparent and homogeneous cathode can be obtained.[239] In fact, the presence of 1 wt% graphene ameliorated the electrocatalytic properties of PEDOT:PSS and the PCE values reached 2.3% and 4.5% for the pristine PEDOT:PSS and PEDOT:PSS/graphene composite, respectively. A similar performance with the same composite material was obtained by Wan et al.[240] In a following paper, Yue et al. further optimized the effectiveness of graphene/PEDOT:PSS composite as cathode:[241] the material was synthesized and deposited by one step electropolymerization of EDOT onto FTO. Despite this technique may seem rapid and low energy demanding, the preparation of PEDOT:PSS/graphene dispersion required high temperature (200 °C) and time (4 h). Once deposited, the electrodes must be dried at 100 °C and the use of such temperature constitutes an issue from the sustainability point of view. Graphene flakes offered lamellar structure with high surface area. The resulting material possessed lots of clusters (see **Figure 8**), that enhanced the adsorption of liquid electrolyte and the number of catalytic active sites for I_3^- reduction. Accordingly, the PCE dramatically increased to a value of 7.86%, better than what observed in other papers.[238–240]

Despite the amelioration of PEDOT:PSS performance provided by the hybridization with graphene, the 2D carbon layer still presented a too low amount of electrocatalytic active sites, leading to poor activity. Several strategies may be successfully used for further enhancing the catalytic properties of graphene, such as chemical functionalization (with the introduction of oxygen-containing groups),[247–251] heteroatom doping,[246] and nanostructuration of graphene-based materials.[242,245]

Lee et al. reported easily water-dispersable graphene dots (GDs) incorporated into PEDOT:PSS.[242] GDs are nano-sized graphene spheres, with unique electronic and optical properties, due to the quantum confinement effect.[243,244] The average dimension was 2.90 nm. This resulted in a highly rough surface, whereas pristine PEDOT:PSS afforded a flat surface, that was disadvantageous for electrocatalytic reaction, as demonstrated by cross section and top view SEM images (Figure 7B). PEDOT:PSS/GDs presented also lower sheet resistance compared to pristine PEDOT:PSS ($1.5 \cdot 10^{-4}$ vs $9.6 \cdot 10^{-4}$ Ω cm, respectively). These improved properties resulted in an increased PCE (7.36% vs 5.14%).

Another graphene-based structure that is highly active is given by graphene nanoplatelets (GNPs). They show good stability and overall features, but poor adhesion onto conducting substrates, such as, FTO glass, especially if a thermal treatment is carried out during cell fabrication. The hybridization of GNPs with PEDOT:PSS may potentially ameliorate the catalytic properties, conductivity, and adhesion behavior of both materials. Kim et al. reported a PEDOT:PSS/GNPs composite deposited by e-spray method.[245] Different amounts, ranging from 0.02 to 1 wt%, were dispersed in the PEDOT:PSS matrix. AFM surface characterization clearly evidenced an increase of the roughness and contact area with the electrolyte (Figure 7C). EIS measurements showed lower R_{ct} as the GNPs concentration increased, reaching an extraordinarily low R_{ct} for in the presence of 1 wt% GnPs: 0.07 Ω cm^2. The PV performance obtained through the *J–V* graphs showed a PCE of 8.33% for the DSSC assembled

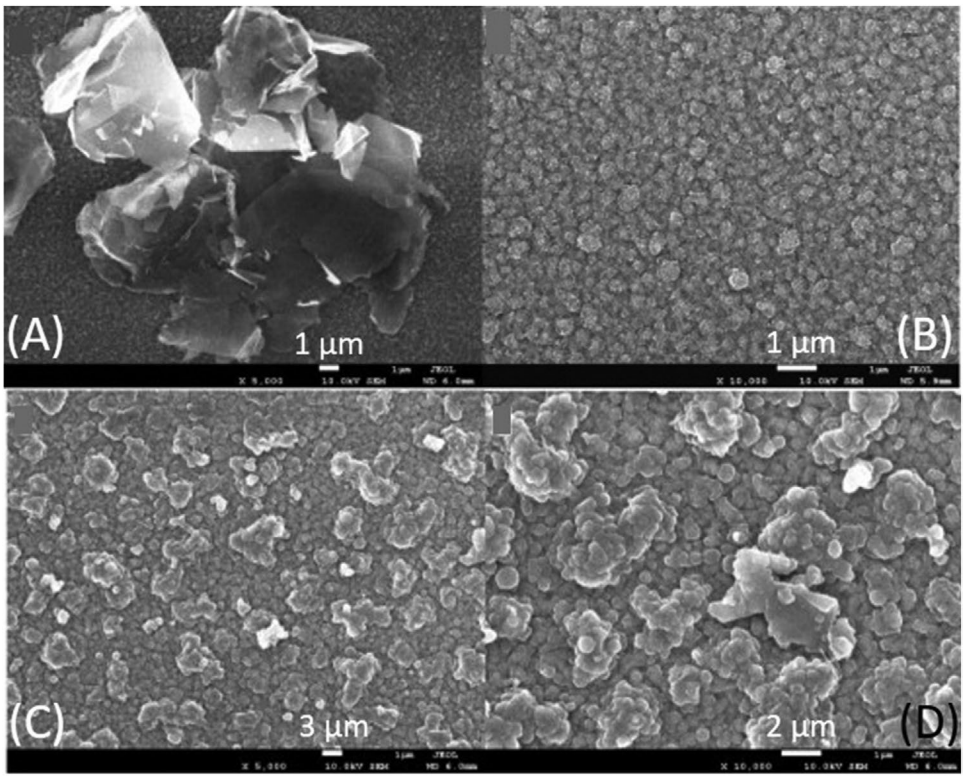

Figure 8. SEM images of A) top-view of graphene flake, B) PEDOT:PSS film, C,D) top-view of the graphene/PEDOT:PSS composite film. Reproduced with permission.[241] Copyright 2013, Elsevier.

with the best sample, better than that obtained with Pt-based cathodes (7.99%).

Nitrogen atoms can be inserted in graphene structure, causing a reorganized resonance phenomenon, which ameliorates its performances. Chen et al. tried to combine the advantages of both PEDOT and N-doped graphene.[246] FESEM images showed that PEDOT was completely decorated with honeycomb-like N-doped graphene structure. A remarkable PCE of 8.30% was obtained. Due to the high transparency of the composite material, a PCE of 6.10% was obtained with back illumination.

3.5.3. Reduced Graphene Oxide and Graphene Oxide

A suitable low cost strategy for obtaining graphene is the chemical oxidation of graphite to produced graphite oxide, followed by exfoliation. Then, a post-reduction treatment is performed to get graphene. In this way, high quality rGO is produced.

Jeong et al. studied the electrocatalytic and charge transfer properties of a counter electrode composed of PEDOT:PSS doped with rGO.[247] To compare the results obtained, they also studied cells with PEDOT:PSS and Pt. FESEM images showed that by adding 10 wt% rGO to PEDOT:PSS increased the surface area and porosity of the layer, with a final thickness of 50 nm. CV measurements showed that PEDOT:PSS/rGO cathode reached better electrocatalytic activity because it produced higher current density than both PEDOT:PSS and Pt. It was found that the addition of rGO improved the activity and morphology of the composite layer. EIS measurements showed that both cathode containing PEDOT:PSS led to higher R_{ct} with respect to platinum, probably due to the lower conductivity of PEDOT:PSS. Despite the higher resistances, the PEDOT:PSS/rGO led to better PCE values, even if with a lower J_{sc} with respect to that of cells assembled with platinum, probably due to the higher resistances.

Sekkarapatti Ramasamy et al. carried out the preparation of a PEDOT/rGO/PPy cathode (PPy = poly(pyrrole)).[248] Large-area GO was obtained by chemical oxidation and then GO/PPy composite was prepared by in situ polymerizzation of pyrrole in GO/sodium dodecylbenzensulfonate aqueous dispersion, followed by a reduction process at 300 °C that lead to rGO. PPy had the role of facilitating the deposition of GO on the glass electrode and was partially destroyed by the thermal treatment. Finally, PEDOT was electrodeposited on the rGO layer (**Figure 9**A). As a main drawback, this synthesis made use of high temperatures, and this point counts when assessing the sustainability aspects. FESEM images revealed a homogeneous dispersion of graphene layer within the PEDOT matrix. Ultraviolet-visible transmittance spectra showed that the rGO/PPy film had good transparency in the visible range. The PV performance were: V_{oc} = 0.76 V, J_{sc} = 17.0 mA cm^{-2}, FF = 0.55, and PCE = 7.1% when PEDOT/rGO/PPy was used, V_{oc} = 0.78 V, J_{sc} = 19.2 mA cm^{-2}, FF = 0.62, and PCE = 9.3% for Pt-based cells.

After the optimization of PEDOT electrodeposition, Li et al. added rGO to increase the conductivity of pristine PEDOT.[249] CV measurements showed that PEDOT/rGO was catalytically more active than other electrodes (e.g., platinum and PEDOT). EIS measurements also confirmed that both R_s and R_{ct} were

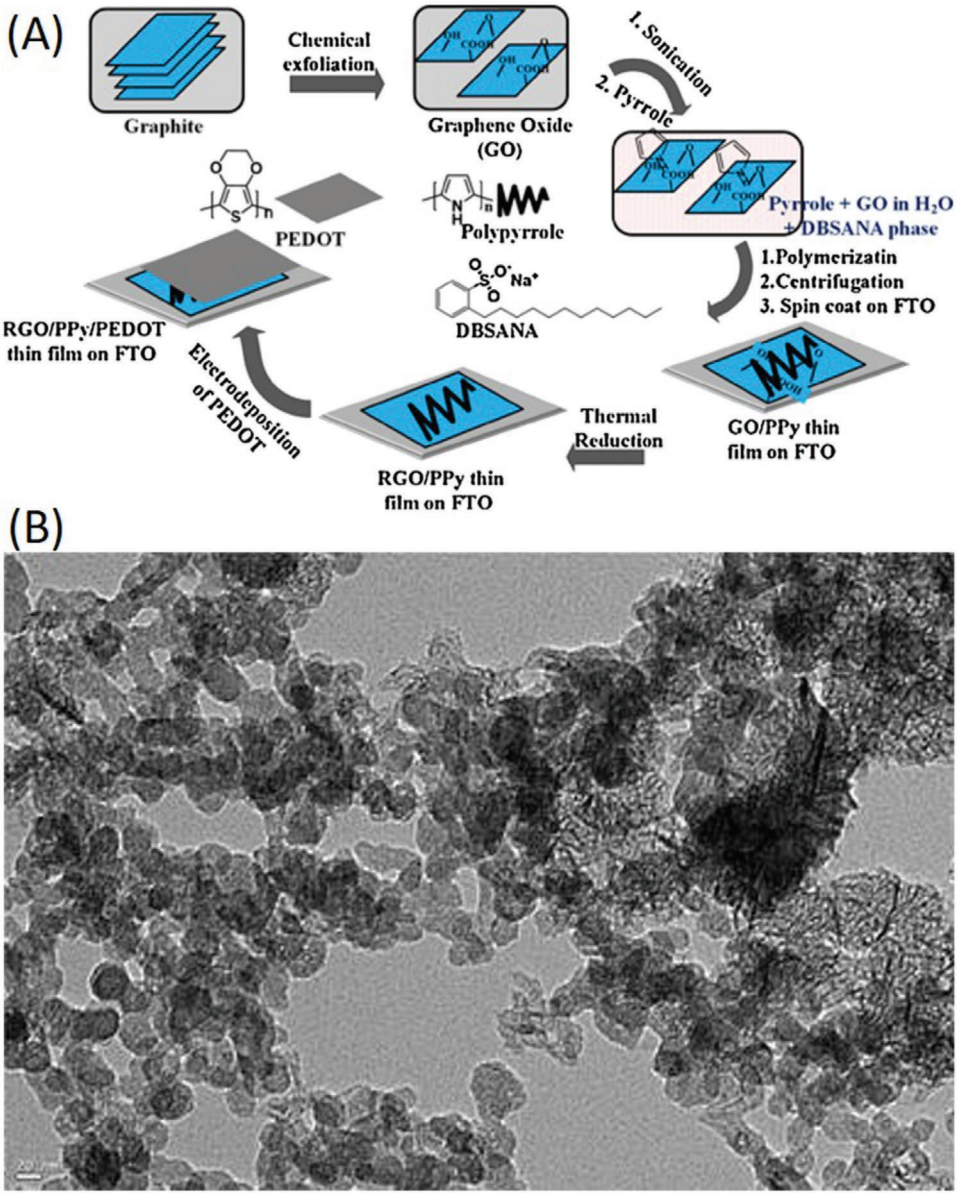

Figure 9. A) Schematic illustration of the fabrication of PEDOT/rGO/PPy counter electrode. First, graphite was exfoliated and partially oxidized to form GO. PPy was in situ polymerized and the GO/PPy composite was deposited on FTO. A thermal reduction treatment at 300 °C was performed to reduce GO and get rGO. Finally, a thin layer of PEDOT was electrodeposited. B) TEM image of SWCNHs. Reproduced with permission.[248,259] Copyright 2015, Elsevier. Copyright 2016, Springer.

lower than those measured with platinum and pristine PEDOT. An overall PCE of 7.12% was obtained.

The electrodeposition strategy was also chosen by Ma et al.[250] As a matter of facts, this strategy is highly reproducible and does not involve the use of high temperature and toxic volatile solvents. The use of binder materials, that could potentially limit the charge transfer, is avoided. The authors reported the facile preparation of a PEDOT/rGO electrode, obtained by electrochemical deposition of PEDOT/GO on FTO glass, followed electrochemical reduction. CV analyses showed that PEDOT/rGO achieved higher catalytic activity than others electrodes. EIS analyses also showed that R_{ct} dramatically decreased from 66.95 Ω cm^2 (PEDOT) to 18.17 Ω cm^2 (PEDOT/rGO), resulting in better electronic transport and higher PCE. The polymerization time was explored between 150 and 250 s; however, in the considered range, PCE did not significantly vary (7.37–7.79%).

Lan et al. performed the H_2SO_4 treatment of PEDOT:PSS/rGO composite.[251] As previously mentioned, the acid treatment can boost the conductivity of PEDOT:PSS polymer.[215] TEM images of both treated and untreated electrodes showed nanocracks; however, after the treatment with H_2SO_4, the transparency of the electrodes increased, due to high homogeneity. The CV analysis demonstrated that, after the acid treatment, the cathodic current peak value increased and peak-to-peak separation decreased, thus confirming the validity of the proposed treatment in enlarging the number of electrocatalytic

active sites. A PCE of 7.07% was obtained for H_2SO_4-treated PEDOT:PSS/rGO, whereas the untreated one achieved a PCE of 3.94%.

3.5.4. Carbon Nanotubes

CNTs are composed by a folded graphene layer and show remarkable features, such as mechanical strength, thermal and chemical stability, high catalytic activity, and electronic properties. For these reasons, they have been intensively studied for optical and electronic applications.[252–254]

Shin et al. reported PEDOT/CNTs with core-shell structure, synthesized by emulsion polymerization;[255] dodecylbenzene sulfonic acid was used as surfactant. When added to water, both CNTs and EDOT precursors associated into micelles; EDOT was then polymerized by the addition of $FeCl_3$. TEM images showed that core-shell nanostructures properly formed and the surface of CNTs was completely covered by a 2–6 nm thick layer of PEDOT. A PCE of 4.62% was reached.

Another key feature to improve conductivity is the orientation at the molecular and nanometric scales of conductive polymers and materials. That is, charge transfer results easier whether the nanostructures are consistently oriented. For this reason, Guan et al. produced aligned CNTs in polymeric composites, by coating PEDOT:PSS on CNTs sheets.[256] The structure formed by CNTs had multi-walled shape, with a diameter of about 10 µm. Subsequently, PEDOT:PSS was spin coated on the CNTs sheet, forming a high quality film and a cathode with high electrocatalytic performance. This aligned composite film featured higher electrocatalytic activity with respect to randomly dispersed CNTs in PEDOT:PSS; EIS measurements also confirmed that both R_s and R_{ct} were much lower. The PCE of the resulting DSSCs doubled that of the unaligned samples (8.3% vs 4.0%, respectively).

Lin et al. manufactured flexible and low cost counter electrodes composed of plasma-etched CNTs/poly(propylene) decorated with PEDOT mixed with CNTs.[257] This also allowed the replacement of TCO. The PV performance of the counter electrode laden with 40 wt% CNTs reached a PCE = 6.82%, comparable to that obtained with Pt-based cathode (7.20%) in the same cell architecture.

Recently, nonlinear CNTs morphologies, such as nanohorns and coiled, were found to increase DSSCs performances.[258] Carbon nanohorns are a kind of nanotubes with tubular structure, dimensions of 2–5 nm in diameter and 30–50 nm in length; they associate into roundish aggregates of 100 nm, with high surface area (300–30 $m^2\ g^{-1}$).[259] The surface area can be further increased up to 1000 $m^2\ g^{-1}$ by oxidation; this reaction opens the horn tip, making that area suitable for electrochemical reactions. Susmitha et al. made a hybrid material by mixing PEDOT:PSS and single wall carbon nanohorns (SWCNHs).[259] TEM images showed that SWCNHs tended to form spherical or boundless aggregates with a diameter of about 10 nm (Figure 9B). Various blend concentrations were tested; the best PCE of 4.70% was reached with a concentration of SWCNHs of 0.3 wt%. The same authors reported, same years later, the same materials in a different configuration;[260] they made a bilayer deposition of SWCNHs over PEDOT:PSS, rather than mechanically mixing the two material. The PCE was improved to a value of 5.10% under the same conditions.

Coiled CNTs exhibited superior electrical and mechanical characteristic when compared to linear CNTs.[258] In particular, the conductivity was enhanced because the coiled shape can enhance the electric field. The coiled shape is due to the presence of hydroxyl or carboxyl groups, due to carbon atom defects. These groups can act as reaction centres and facilitate the dispersion of coiled CNTs in water. Yun et al. made the hybrid material with coiled CNTs and PEDOT:PSS and treated it with methanol and HCl to further increase the performance;[258] the highest PCE was 5.3%.

Zhang et al. prepared the composite PEDOT/MWCNTs by simple and reproducible oxidative electropolymerization method on FTO glass.[261] The studied samples differed for the adopted deposition charge (5, 25, 100, 200, 400 mC cm^{-2}). Through SEM analysis, it was noted that MWCNTs-PEDOT showed higher porosity and that the thickness of the film increased with the deposition charge. CV measurements revealed that the electrocatalytic activity of PEDOT/MWCNTs composite was much higher than that of pristine PEDOT and this was due to the increase of active sites. Therefore, the PCE shifted from 4.84% to 5.47% for pristine PEDOT- and PEDOT/MWCNTs-based devices, respectively. The PCE was further increased (6.67%) some years later by Rhee et al., who prepared a PEDOT:PSS/MWCNTs composite by CV.[262] Xiao et al. adopted an analogous electrodeposition method, but with the potentiostatic pulse technique, to prepare a PEDOT/MWCNTs composite.[263] In this way, MWCNTs assumed a fiber-like morphology, whereas the PEDOT formed a nanomeadow. As a result, the PCE was further increase to 7.03%.

Lee et al. improved the performance of PEDOT/MWCNTs composite, by acting on the chemical oxidative synthesis of PEDOT.[264] They added imidazole to the EDOT precursor; this molecule reduced the reactivity of $Fe(OTs)_3$ (OTs = toluenesulfonate) oxidizing agent, slowing down the reaction rate. Without imidazole, the fast kinetics brought to crack and formation of isolated droplets. However, with the addition of imidazole, the resulting layer was thicker, dense, and more uniform. The addition of MWCNTs further enhanced the electrocatalytic activity of conductive PEDOT, allowing a PCE of 8.08%. A deeper investigation was performed by Yun et al., who investigated the effect of MWCNTs dispersed into PEDOT:PSS.[265] The concentration of MWCNTs ranged between 0.05 and 0.3 wt% in the PEDOT:PSS solution. The highest PCE (6.0%) was reached with 0.3 wt%, since the surface area and electrocatalytic properties of the electrode increased linearly with the amount of MWCNTs. However, higher concentration of MWCNTs did not bring to a processable homogenous film and could not be used for preparing counter electrodes. The main differences in PCE with respect to the work of Lee et al. may be attributed to the use of different dyes (i.e., N3 and N719), the presence of different PEDOT counteranions (i.e., OTs^- and PSS^-) and the use of a different synthetic pathway (i.e., chemical oxidation and spin coating of commercial PEDOT:PSS water dispersion).

More recently, Li et al. exploited the transparency of MWCNTs and honeycomb-like PEDOT for bifacial DSSCs and compared it with bifacial flat PEDOT.[266] Five types of counter electrodes were tested: flat PEDOT, flat PEDOT/MWCNTs, honeycomb-like PEDOT, honeycomb-like PEDOT/MWCNTs, and platinum. PV parameters indicated that the PCE shifted

from 8.10% to 9.07%, passing from flat to honeycomb-like PEDOT/MWCNTs.

3.6. Poly(3,4-ethylenedioxythiophene) Hybridized with Other Materials

3.6.1. Poly(3,4-ethylenedioxythiophene) + TiO_2

The surface area of ion-doped PEDOT/FTO is still low if the aim is that of implementing its use as counter electrode. For this reason, Sakurai et al. deposited a thin layer of TiO_2 particles between PEDOT and FTO.[267] TiO_2 positively changed the interfacial electron transfer and, as a result, it had a beneficial effect on cell performance; also, R_{ct} turned out to be lower with respect to the pristine counterpart. However, the overall PCE values were still low (below 5%) and further improvements were still necessary.

Differently, Maiaugree et al. mixed TiO_2 NPs within the PEDOT matrix and studied the effect of particles concentration on cell performance.[268] The addition of small NPs is a known strategy to increase the surface area and film roughness of PEDOT flat films, thus enhancing—in this case—the interfacial contact with the I-based liquid electrolyte. The effect was confirmed also by SEM characterization. The DSSCs showed very high performance, with PCE of 8.49%, higher than obtained for cells assembled wit sputtered platinum (7.5%) and pristine PEDOT:PSS (5.27%). This performance improvement was related to the decrease of the R_{ct}: TiO_2/PEDOT:PSS composites showed R_{ct} values ranging from 1.3 to 11 Ω, depending on the amount of TiO_2 NPs, while that of pristine PEDOT was 55 Ω. An analogous PEDOT:PSS/TiO_2 composite was realized by Jafari et al.; however, in this case the PCE was very low (below 1%).[269] Seo et al. studied the effect of TiO_2 NPs concentration in PEDOT:PSS dispersion (from 10 to 200 mg mL^{-1}) as well.[270] AFM images showed that, after the addition of NPs, the surface of PEDOT:PSS increased in roughness and porosity, thus also raising the surface area, indicating an improvement of catalytic performance. CV tests showed that, as the amount of TiO_2 increased, the cathodic current density reached a maximum when 200 mg mL^{-1} TiO_2 was used. EIS tests also confirmed that 200 mg mL^{-1} was the best compromise for lower resistance and impedance. The PV performance confirmed the results obtained from the previous tests, obtaining these values: V_{oc} = 0.72 V, J_{sc} 16.39 = mA cm^{-2}, FF = 0.72, and PCE = 8.27%; for Pt-based cells, values were: V_{oc} 0.73 V, J_{sc} 14.75 mA cm^{-2}, FF = 0.71, and PCE = 7.59%.

Song et al. studied the effect of the addition of Si, TiO_2 and SiO_2 NPs to PEDOT as well.[271] These materials had different specific surface area, that is, SiO_2 > TiO_2 > Si. SEM images showed that all three films were mesoporous, with a higher surface area than that of pristine PEDOT:PSS, resulting in better electrocatalytic activity. The PCE followed the trend of the surface area: SiO_2 (6.9%) > TiO_2 (6.8%) > Si (5.7%). PEDOT/TiO_2 had the highest V_{oc} (0.75 V) due to the large conduction band of TiO_2, that improved the charge transfer. However, PEDOT/SiO_2 led to cells with the highest FF, and this clarified the highest PCE. Song et al. exploited the properties of nanosized SiO_2 to enlarge the surface area of PEDOT counter electrodes.[272] Nanosized SiO_2 also had the advantages of being transparent in the visible range; however, a lower PCE of 4.61% was obtained.

Xu et al. further improved the contact of PEDOT:PSS/TiO_2 composite with FTO substrate by adding SnO_2 particles (**Figure 10**A).[273] TiO_2 NPs were placed in an aqueous solution with $SnCl_4$, then coated onto a conductive substrate and heated up to 150 °C to form a conductive layer as a template on which PEDOT:PSS was deposited. $SnCl_4$ was transformed into the oxide during the thermal treatment in air. The addition of SnO_2 was effective in improving the contact with the substrate; the resulting composite layer showed good conductivity, nanoporous structure and mechanical strength. The PV performance confirmed the superiority of PEDOT:PSS/TiO_2/SnO_2 cathode, obtaining a PCE of 6.54%, higher than that of pristine PEDOT:PSS-based DSSCs (4.79%).

Mustafa et al. combined the positive effects of both TiO_2 and GO in increasing the surface area and the catalytic activity of PEDOT-based CEs.[274] The morphology was studied by FESEM analysis and it was observed that PEDOT showed dense, granular and wrinkled morphology; PEDOT-GO had a uniform morphology with paper-like sheet resembles contributing to an increase in surface area; PEDOT-GO/TiO_2 showed a porous surface with spherical NPs and paper-like sheet morphology. CV measurements showed that PEDOT-GO/TiO_2 had much higher cathodic current densities than PEDOT-GO and platinum (−5.49, −3.57, and −3.54 mA cm^{-2}), thus confirming its superiority in electrocatalytic activity. PEDOT-GO/TiO_2 counter electrodes resulted the best both in terms of PV performance and internal resistances (R_s and R_{ct}).

3.6.2. Poly(3,4-ethylenedioxythiophene) and Other Oxides

Well-aligned PEDOT nanostructures with good adhesion to the substrates are necessary to improve PV performances. A suitable strategy for reaching this target is the use of templating agents, such as anodic Al_2O_3. Kung et al. used ZnO nanorods as a template for the deposition of PEDOT;[275] after the deposition, ZnO can be easily removed by dissolving it in acid solution. Consequently, PEDOT with hollow microflowers morphology was obtained and the best PCE was 7.20%.

Among other metal oxides, Fe_3O_4 was deeply studied due to its strong catalytic activity, low cost, and high conductivity. Zheng et al. reported a PEDOT/Fe_3O_4 composite, obtained by in situ polymerization.[276] The amount of Fe_3O_4 was varied between 0 and 3 mg mL^{-1} with respect to the EDOT precursor solution. The best PV parameters were reached with a concentration of 2 mg mL^{-1} (0.740 V, 18.6 mA cm^{-2}, 0.63, 8.69%), that was the best trade-off between electrocatalytic activity and conductivity.

The combination of metal oxides, C-based materials and PEDOT:PSS resulted in a synergistic effect that produced good counter electrodes for DSSC applications, as reported by Mustafa et al.[274] Some years later, Wan Khalit et al. adopted the same strategy, by mixing Al_2O_3, PEDOT, and rGO.[277] The composite counter electrode was prepared by a two-step process: deposition of Al_2O_3-rGO by CV and deposition of PEDOT onto Al_2O_3-rGO by chronoamperometry. The first one was conducted in water between –1.5 and 1.2 V, twice; the second took place in acetonitrile, using $LiClO_4$ as a supporting electrolyte for 100 s.

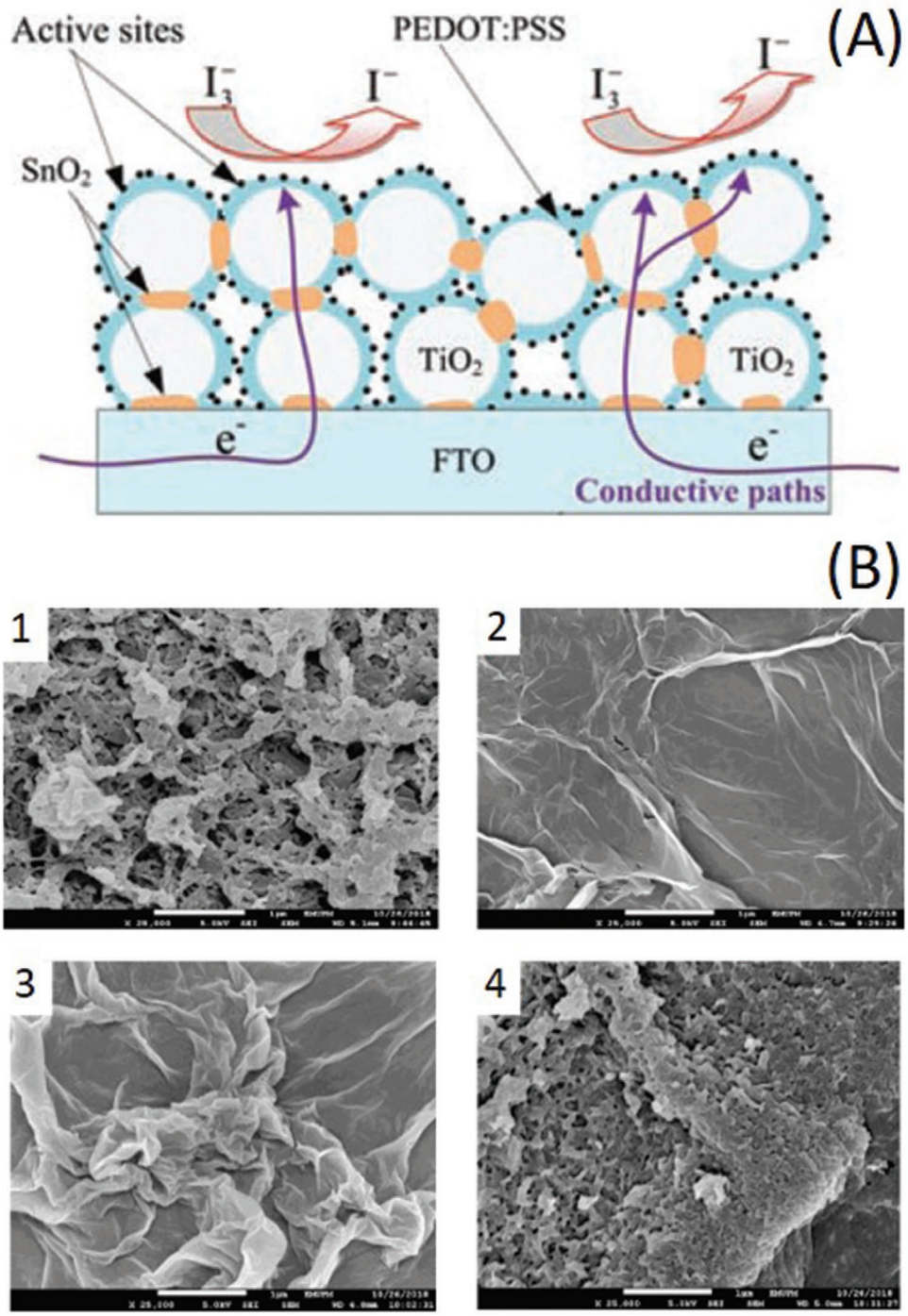

Figure 10. A) Microstructured model for PEDOT:PSS/TiO_2/SnO_2 composite, highlighting the good adhesion to the FTO and the electron path. B) FESEM images of 1) pristine PEDOT, 2) pristine rGO, 3) PEDOT-rGO, and 4) PEDOT-rGO/Al_2O_3. Reproduced with permission.[273,277] Copyright 2016, American Scientific Publishers. Copyright 2019, Elsevier.

FESEM images showed that the PEDOT/Al_2O_3-rGO composite layer had the wrinkled paper-like structure typical of rGO and a coral-like structure typical of PEDOT, with distributed Al_2O_3 NPs increasing the presence of active sites (Figure 10B). Overall, the layer showed high porosity, resulting in high surface area. However, the PCE was still low (2.15%) with respect to other literature reports, due to low FF and quality of the interface.

3.6.3. Poly(3,4-ethylenedioxythiophene) and Sulfides, Nitrides and Carbides

Metallic compounds such as nitrides,[278,285] sulfides,[280,285] and carbides[279] were studied due to their noble metals-like properties. The hybridization of these metallic compounds in the form of NPs with conductive polymers represents a suitable

strategy to avoid their aggregation and exploit the overall superior catalytic activity.

As an example, Xu et al. reported a counter electrode based on a PEDOT:PSS/TiN composite, made by facile mixing, followed by ultrasonic treatment; in particular, the authors used three different morphologies, that is, NPs, nanorods and mesoporous spheres.[278] NPs were better dispersed on the surface of the PEDOT:PSS. It was noted that nanorods- and NPs-based samples showed electrocatalytic properties comparable to those of platinum; *J–V* tests confirmed the excellent performance of the corresponding DSSCs, which reported PCE values of 7.06% and 6.89%, respectively, higher than those of Pt-based devices, which reached 6.57%. Conversely, PEDOT:PSS/TiN mesoporous spheres led to a PCE = 6.19%.

Among carbides, SiC has the potentially of replacing platinum, due to its low cost and high activity. Tsai et al. studied a cathode composed of PEDOT:PSS doped with SiC NPs.[279] When SiC NPs were added to PEDOT:PSS, the surface became porous and showed a high surface area and a good adhesion to ITO substrates. PV performance confirmed that cells with PEDOT:PSS/SiC-NPs reached PCE close to those of Pt-based counterparts, that is, 7.25 and 7.98%, respectively.

Among sulfides, CoS shows remarkable properties and good transparency as well. Sudhagar et al. reported the use of CoS NPs mixed within a PEDOT:PSS matrix.[280] CoS increased the performance of the counter electrode material, as demonstrated by the high current density peak obtained from CV measurement. The PV performance showed high PCE (5.4%), even if slightly lower than that of Pt-based cells (6.1%). They also noted that the J_{sc} of PEDOT:PSS/CoS-based cells was higher than that of pristine PEDOT:PSS-based ones (13.2 and 11.6 mA cm^{-2}, respectively), and even higher than that of Pt-based devices (13.0 mA cm^{-2}). However, the use of cobalt in DSSCs remains controversial, due to its scarcity, toxicity, and unfair distribution.[20]

As for TiN, also its corresponding sulfide (TiS_2) has been used in various electronic devices, due to its interesting properties, such as, high conductivity and electrocatalytic activity.[281,282] For these reasons, Li et al. made a PEDOT:PSS/TiS_2 composite, to overcome the fact that bare TiS_2 is commonly obtained in the form of particles with average size of 1 μm and with little contact with ITO substrates.[283] PEDOT:PSS/TiS_2 composite presented high roughness and improved surface area, and the resulting devices reached a PCE of 7.04%, much higher than that of pristine PEDOT:PSS.

One of the most studied sulfide is MoS_2. Typically, MoS_2 possesses a 2D layered structure with poor exposure of active sites. For this reason, several strategies for increasing the number of active sites have been proposed, for example, MoS_2 can be easily dispersed in PEDOT:PSS-based solutions. The polymer itself is able to reduce the restacking of the material, without compromising both the catalytic and conductivity properties. With this idea, Song et al. mechanically dispersed MoS_2 in PEDOT:PSS;[284] they used MoS_2 with different dimensions (i.e., 100 and 30–40 nm, respectively). *J–V* measurements showed that cells assembled with the cathode consisting of PEDOT:PSS/MoS_2(30–40 nm) reached a higher PCE (5.7%) than those fabricated with PEDOT:PSS/MoS_2(100 nm) (4.7%).

In a similar way, Ahmed et al. made a composite material with MoS_2 and Si_3N_4.[285] In fact, the combination of semiconductor materials was demonstrated to diminish the stacking between layers and enhance the catalytic activity of MoS_2. In addition, the blending with conductive PEDOT:PSS ameliorated the adhesion to the substrate, without sacrificing the electronic conductivity. EIS characterization demonstrated the strong reduction of R_{ct} for the composite material and an overall 7.22% PCE was achieved.

Xu et al. reported a transparent counter electrode made by a layer of MoS_2 on FTO, subsequently covered by PEDOT.[286] MoS_2 was synthesized by hydrothermal method, whereas PEDOT was deposited by electropolymerization. The film of PEDOT/MoS_2 showed a different morphology from that of pure PEDOT, with very small pores and good uniformity, which increased the surface area exposing many active sites. In this way, they created a good bifacial device (**Figure 11**A), with PCE = 7.0% (front illumination) and 4.82% (back illumination).

Table 1 summarizes the most relevant results obtained with PEDOT-based counter electrodes in the DSSCs field.

4. Poly(3,4-ethylenedioxythiophene) as Hole-Transporting Material for Solid-State Dye-Sensitized Solar Cells

4.1. Deposition Techniques and Performances

PEDOT finds application also as a replacement for redox shuttle-based electrolytes in DSSCs, due to its good charge transfer properties (conductivity = 550 S cm^{-1}),[287] low cost and easy processability. In addition, it forms a film transparent in the visible range; therefore, any possible competition for light absorption with the dye is avoided. This is of crucial interest for tandem and/or bifacial devices.

According to the best of our knowledge, Saito et al. were the first authors reporting the use of PEDOT as HTM in the DSSCs field.[287] They carried out in situ polymerization of EDOT precursor on dye-sensitized TiO_2, in order to facilitate the contact between the photoanode and the HTM. Indeed, the proper permeation of the HTM within the mesoporous TiO_2 is necessary to ensure a good contact with the dye and to minimize recombination at the dyed photoanode/HTM interface. The cell gave a very low PCE of 5.4×10^{-3}%. To improve this performance, 1-ethyl-3-methylimidazolium bis((trifluoromethyl)sulfonyl) amide ionic liquid and 4-*tert*-butylpyridine (TBP) were added as additives, leading to a reduction of the charge recombination. However, the PCE remained quite low (8.5×10^{-3}–1.2×10^{-2}%). To further reduce the charge recombination, the same authors tried to use an amphiphilic ruthenium dye with long chains, that is, *cis*-RuLL′(SCN)$_2$ (Z907), with L = 4,4′-dicarboxylic acid-2,2′-bipyridine and L′ = 4,4′-dinonyl-2,2′-bipyridine, by adopting the same cell architecture.[288] Z907 dye gave PCE values almost doubled with respect to those provided by N719 (0.67 vs 0.31%, respectively). At the same time, a thin layer of compact Al_2O_3 was deposited onto the mesoporous TiO_2 before dye adsorption; this layer drastically reduced the dark current, so the PCE further increased up to 0.93%. The charge transport process in

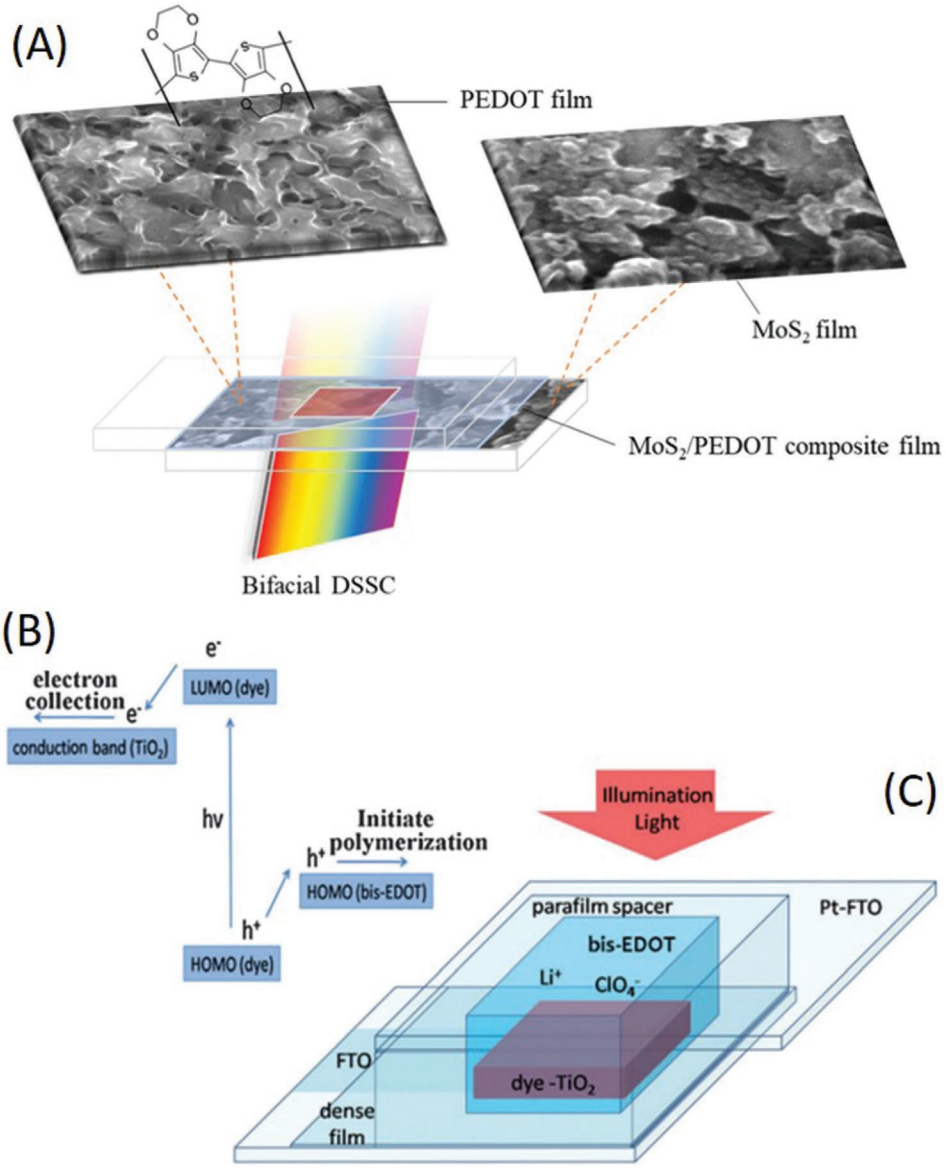

Figure 11. A) Schematic illustration of a bifacial DSSC, with PEDOT/MoS_2 composite as transparent cathode. B) Schematic representation of PEP mechanism and relative thin layer electrolytic cell. Reproduced according to the terms of the CC-BY license.[286] Copyright 2020, The authors. Reproduced with permission.[295] Copyright 2012, RSC.

PEDOT-based systems was further analyzed by stepped light-induced transient measurement of photocurrent and photovoltage[289] and compared with that of corresponding liquid electrolytes based on iodide/triiodide redox shuttle. Such characterization demonstrated that photovoltage decay, in PEDOT-based devices, was faster than in I-based cells and electron lifetime was 10–30 times shorter. Also, EIS showed that the total impedance of PEDOT-based cells was higher than that of the I-based DSSCs. Overall, this study highlighted the importance of the PEDOT/photoanode interface, to ensure good dye regeneration efficiency and avoiding charge recombination phenomena.

Another step forward in this field was reported by Kim et al.[290] PEDOT was prepared by photoelectropolymerization (PEP) on Z907-sensitized TiO_2. *bis*-EDOT precursor was pre-deposited onto a mesoporous TiO_2 layer and the electropolymerization was accompanied by visible light irradiation. Indeed, after the light absorption by the dye molecule, hole-electron pairs are formed; while electrons are injected into the TiO_2 conduction band, the holes carry on the polymerization process, as shown in Figure 11B. The main advantages of PEP technique are the long permeation depth, the good interfacial contact between dyed-anode and the hole conductor and the full coverage of TiO_2 photoanode.[295] In addition, the rapidity and the low energy-demand make PEP suitable for large scale applications. It was demonstrated that this procedure yields to better performance, by creating a better interface between dye and conducting polymer.[289,291–293] Therefore, the choice of the photosensitizer strongly affects the morphology and properties

Table 1. Overview of PEDOT-based counter electrodes for DSSCs, listing the most innovative concept of each publication and the corresponding PCE value measured under 1 sun irradiation.

	CE	PCE [%]	Ref.
Pure PEDOT	PEDOT	7.82	[189]
	Synthesis in aqueous medium	6.46	[195]
	Spin coating deposition of EDOT and annealing	7.04	[197]
	Oxidative molecular layer deposition	7.18	[198]
	Nanostructured PEDOT morphology	8.3	[202]
	Honeycomb-like PEDOT morphology	9.12	[205]
	NF PEDOT morphology	9.2	[203]
PSS-doped	Annealing treatment of PEDOT:PSS (45–60 °C)	3.22	[212]
	PEDOT:PSS	4.10	[209]
	PEDOT:PSS on flexible substrate	4.84	[190]
	Annealing treatment of PEDOT:PSS (80–120 °C)	6.37	[214]
	Solvent treatment of PEDOT:PSS	7.29	[216]
	HNO_3 treatment of PEDOT:PSS	8.61	[215]
Anion-doped	Different counteranions (ClO_4^-, TsO^-, PSS^-)	4.0–4.2	[218]
	PEDOT:TsO	4.60	[219]
	PEDOT:TsO treated with hydrazine and iodine	6.86	[221]
Modified	Metal cations (Mn^{2+}, Co^{2+}, Ni^{2+}, Cu^{2+}) doping	5.19	[226]
	Cationic ammonium moiety and iodide as counterion	6.64	[227]
	PEDOT-g-PEG	8.45	[225]
With graphite/carbon	PEDOT/carbon nanosphere	6.5	[231]
	PEDOT/bio-derived carbon	6.54	[234]
	PEDOT/graphite/carbon black	7.01	[228]
	PEDOT/exfoliated graphite	8.0	[233]
With graphene and rGO	PEDOT:PSS/graphene (electrodeposition)	4.5	[241]
	H_2SO_4-treatment of PEODT:PSS/rGO	7.07	[251]
	PEDOT:PSS/GDs	7.36	[242]
	PEDOT/rGO	7.79	[250]
	PEDOT/N-doped graphene	8.30	[246]
	PEDOT:PSS/GNPs	8.33	[245]
With CNTs and MWCNTs	PEDOT/CNTs	4.62	[255]
	PEDOT:PSS/CNT nanohorns	4.70	[259]
	Plasma-etched CNT/poly(propylene) decorated with PEDOT	6.82	[257]
	PEDOT/MWCNTs (electrodeposition)	7.03	[263]
	PEDOT:PSS coated on aligned CNTs	8.3	[256]
	Honeycomb-like PEDOT/MWCNTs	9.07	[266]
With TiO_2/oxides	PEDOT/TiO_2/SnO_2	6.54	[273]
	PEDOT/SiO_2	6.9	[271]
	PEDOT/TiO_2	8.49	[268]
	PEDOT/Fe_3O_4	8.69	[276]
With sulfides, nitrides and carbides	PEDOT:PSS/CoS	5.4	[280]
	PEDOT:PSS/MoS_2	5.7	[284]
	PEDOT:PSS/TiS_2	7.04	[283]
	PEDOT:PSS/TiN	7.06	[278]
	PEDOT:PSS/MoS_2/Si_3N_4	7.22	[285]
	PEDOT:PSS/SiC	7.25	[279]

of the resulting layer. PEDOT was doped with 1-butyl-3-methylimidazolium bis(trifluoromethansulfonyl)amide, lithium bis(trifluoromethanesulfonyl)amide (LiTFSI), and TBP to avoid recombination. Under optimized condition, a PCE of 2.62% was achieved.

Mozer et al. studied the effect of the duration of PEDOT deposition under the same conditions;[294] PEP time was varied between 4 and 30 min. The authors further investigated the kinetics of dye regeneration, through the transient absorption measurements, and compared it with that of traditional spiro-MeOTAD and I-based redox couple in acetonitrile/valeronitrile liquid electrolyte. It was found out that the regeneration of $Z907^+$ occurred in 1–100 μs with PEDOT as HTM; this time was orders of magnitude lower than that of traditional spiro-MeOTAD (ps to ns) and that of liquid I^-/I_3^- electrolyte (ns to μs). The slow regeneration time limited the PCE as well. In fact, the best PCE of 3.0% observed for PEDOT-based cells was still far from that of traditional I-based electrolytes.

Organic dyes seem to provide a more efficient interplay with PEDOT, as demonstrated by Liu et al.[138] Fully organic D149 dye was used to replace Ru-based complex Z907 and a remarkable PCE of 6.1% was achieved, that was well superior to what reached in the previous studies on PEDOT as HTM.

Since PEP process is initiated by the creation of a hole in the HOMO level of the dye molecule and different dyes absorb in different radiation ranges, the wavelength of PEP process represents a fundamental aspect, that can alter the resulting PEDOT layer performances in cells. Liu et al. studied for the first time the influence of the wavelength (740, 670, 605, and 540 nm) of the incident radiation used during the preparation procedure on the cell performance.[295] The PCE increased with the irradiation wavelength, with a maximum occurring at 670 nm, where PCE = 7.1%. This value was even higher than what reached with continuous light radiation. In fact, at 740 nm the absorbance of the dye drastically decreased: few holes were formed and PEDOT was obtained by traditional electropolymerization. Therefore, the maximum PCE can be reached by irradiating at a wavelength where the light absorption of the dye is maximized.

Later, Park et al. studied the influence of light intensity during PEP on the corresponding device performance and investigated the hole transfer mechanism in these cells.[296] PEDOT film was formed at three different light intensity values: 0.01, 0.1, and 0.3 sun. At low light intensity, the film was more homogeneous, due to the lower nucleation rate, and the polymer possessed a higher chain length. On the other hand, at high light intensity the film was brittle, with a less coverage of mesoporous TiO_2 and with a shorter chain length. Moreover, both samples presented ionic species, such as polarons ($PEDOT^+$) and bipolarons ($PEDOT^{++}$), as demonstrated by the presence of the corresponding peaks in the near-infrared/visible/ultraviolet spectrum. Looking at the photoinduced absorption spectroscopy (PIA), the authors suggested that dye regeneration was mainly due to the hole transfer from the dye to PEDOT polarons, with the formation of PEDOT bipolarons. These charges involved in the cell operation can be better delocalized and stabilized in a longer chain polymer. For this reason, the PCE values of the corresponding devices decreased with the light intensity used during PEP; they were 2.5% (0.01 sun), 2.0% (0.1 sun), and 1.3% (0.3 sun).

One the major disadvantages of PEP is the use of volatile organic solvents. Zhang et al. were the first reporting a PEP process carried out in an aqueous micellar medium.[297] This strategy was more environmentally friendly and decreased the oxidation potential of *bis*-EDOT precursor, since the onset oxidation potential in the aqueous phase was 0.3 V lower than that commonly used in acetonitrile, making the process easier. In particular, the authors performed a traditional PEP in acetonitrile and in water, facilitating the dissolution of *bis*-EDOT by using surfactants. The PEDOT layer originated from organic PEP assumed a smooth and compact morphology, with long polymer chains. On the other hand, the PEDOT obtained from aqueous media was rough and highly porous, with shorter polymer chains. The PCE values reached were comparable, that is, 5.6 and 5.2% for organic and aqueous phases, respectively. Further characterization, such as PIA and near-infrared/visible/ultraviolet spectroscopy, revealed that the aqueous-derived PEDOT provided better dye regeneration, but faster charge recombination. Therefore, the cell PCE was confirmed to be the best trade-off between these two phenomena.

Considering the whole DSSC operating process, the TiO_2 particle dimensions is fundamental as well, as shown by Zhang et al.[298] In fact, larger pore sizes provided a favorable insertion pathway of *bis*-EDOT precursor, making PEP more efficient. On the other hand, a smaller pore size may ensure a better interface between dye and HTM, thus facilitating the dye regeneration process. The authors synthesized TiO_2 particles by a modified sol–gel procedure and compared the performance of the corresponding device to the TiO_2 particles obtained by a commercial Dyesol paste. Under optimized conditions, a PCE of 5.2% was achieved, slightly higher than that reached starting from commercial TiO_2 (4.5%).

Overall, this section highlights that the preparation process of PEDOT-based HTMs strongly contributes to the final DSSC performance. The chronological overview offered above clearly shows how the scientific community tried to improve the electrode/HTM interface and it definitely emerged that tuning PEP protocols is a valid strategy to boost PCE values. On the other hand, long-term stability studies are missing in the vast majority of literature reports, thus leaving unclear if DSSCs durability is effectively improved with respect to liquid and quasi-solid systems.

4.2. Anion-Doped Poly(3,4-ethylenedioxythiophene) and its Hybridization

More recently, many strategies for improving the PCE values of PEDOT-based DSSCs have been proposed, such as, anion-doping[293,299,300] and hybridization.[302,303] Generally speaking, the anion doping increases the overall conductivity of PEDOT, an aspect of paramount importance for an efficient HTM; however, the probability of cell short-circuit should be avoided lowering any relevant electronic conduction contribution.

Xia et al. explored in details the effect of the counter anion during PEP synthesis, by using different lithium salts, for example, $LiClO_4$, $LiBF_4$, LiTFSI, and $LiCF_3$-SO_3.[293] It was

demonstrated that the anion had a strong effect on cell performance, as shown in the *J–V* curves shown in **Figure 12**A. The PCE followed this trend: $TFSI^-$ (2.85%) > $CF_3SO_3^-$ (2.15%) > ClO_4^- (1.8%) > BF_4^- (0.9%). In fact, PEDOT:TFSI afforded the lower R_s and the highest conductivity and charge transfer effectiveness. This could be partially ascribed to the charge delocalization in the anion, which avoided pairing with Li^+ cation, that could cause a slowing down of the charge transfer.

The influence of the counter anion was further investigated in another study,[299] where anions with different perfluoroalkyl chain length values were analyzed. In particular, both perfluorosulfonates ($CF_3SO_3^-$, $C_4F_9SO_3^-$, $C_8F_7SO_3^-$) and bis(perfluorosulfunyl)imides ($N(CF_3SO_2)_2^-$, $N(C_2F_5SO_2)_2^-$, $N(C_3F_7SO_2)_2^-$, $N(C_4F_9SO_2)_2^-$) were studied. Differently from what expected on the basis of the previous results,[293] the PCE values decreased by increasing the carbon atoms on the alkyl chain (Figure 12B). In fact, the perfluoroalkyl anions may have a drastic influence on PEDOT growth mechanism, reducing the effective contact with TiO_2 photoanode. In addition, the bigger dimension of ions may also decrease the mobility.

Similar PCE values were obtained by Lee et al. as well.[300] In their work, PEDOT was doped with traditional PSS to get PEDOT:PSS, to enhance the electronic conductivity and increase the water dispersion ability. Furthermore, PEDOT:PSS was mixed with glycerol to reduce the resistivity of the layer. In fact, it was previously demonstrated that the addition of polyalcohol to PEDOT:PSS can increase the conductivity without scarifying the optical properties.[301] Under optimized conditions, the best PCE was 2.62%.

PEDOT:PSS was also hybridized with biomolecules and bioderived polymers, such as, deoxyribonucleic acid.[302] This latter is a complex biopolymer, with many heteroatoms able to form complexes with ions. For this reason, it can be applied in optoelectronic devices. However, the reported performances in DSSC are still low (far below 1%). κ-carrageenan is another type of negatively-charged polymer that can be successfully mixed with PEDOT.[303] This biopolymer is a sulfonated polysaccharide, rich in heteroatoms. Ng et al. studied a PEDOT/κ-carrageenen composite as HTM,[303] investigating different amounts of biopolymer (i.e., 0.1, 0.2, and 0.5 wt%). The composite surface was wrinkled and with a higher surface area with respect to the two components considered separately. Conductivity was also measured, and it was observed that, as the amount of κ-carrageenan increased, it increased up to a maximum of 16.23 S cm^{-1} in the presence of 5 wt% κ-carrageenan. However, PV performance showed poor results, with PCE values below 1%, which were attributed to the highly stiff system, impeding efficient charge transportation.

In the previous section, the enhancement of PEDOT conductivity by the hybridization with C-based materials was illustrated. Such materials were also employed as HTMs, as reported by Li et al.[304] In particular, PEDOT was hybridized with graphene and graphene/PtCo. The composites were embedded in a poly(acrylic acid)/PEG (PAA/PEG) matrix. PAA/PEG helped the formation of a 3D network, without compromising both optical and electrical properties of the composites. CV measurements showed that the catalytic properties were improved by switching from PEDOT to PEDOT:graphene and PEDOT:graphene/PtCo alloy NPs.

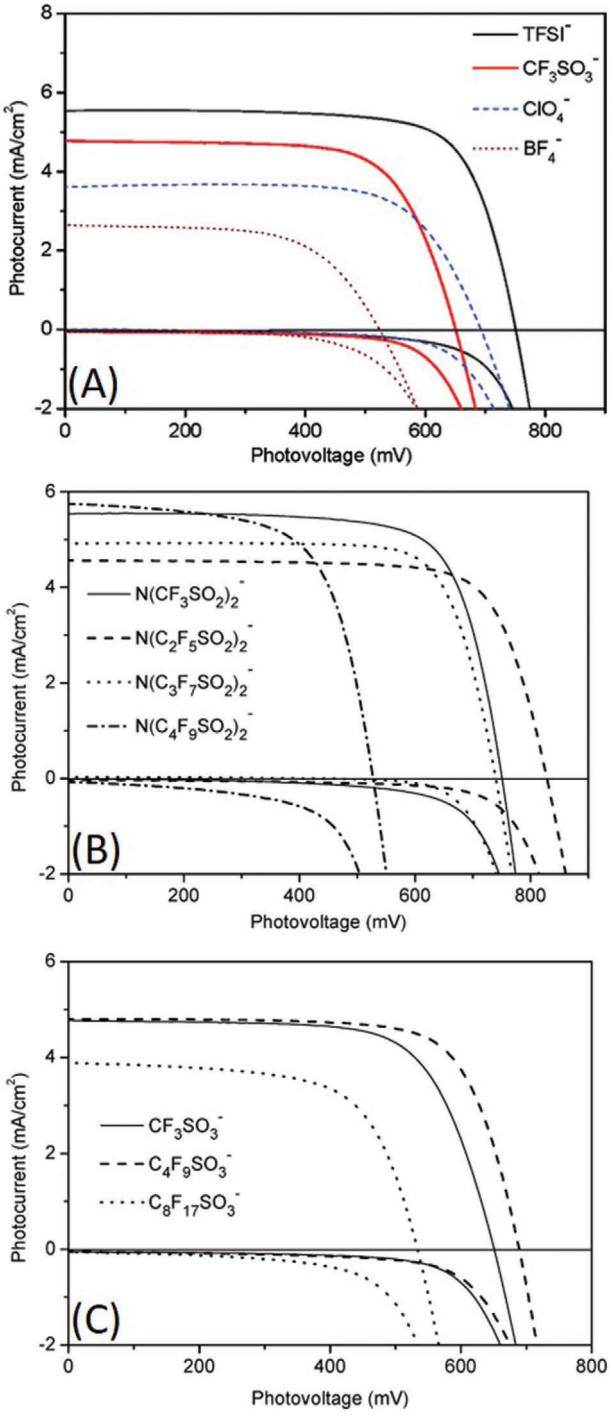

Figure 12. *J–V* curves of DSSCs based on photoelectrochemically deposited PEDOT as HTM bearing A) different anions, B) bis(perfluorosulfunyl) imides, and C) perfluorosulfunates. Reproduced with permission.[293,299] Copyright 2003, ACS. Copyright 2008, ACS.

As a result, the reduction of peak current intensity, reduction potential and peak separation showed that the samples based on PEDOT:graphene/PtCo alloy NPs reached the best performance. Furthermore, this HTM presented the lowest R_s and a remarkable PCE of 8.2% was achieved (vs 5.5% for the undoped-PEDOT).

Table 2. Overview of PEDOT-based HTMs for DSSCs, listing the most innovative concept of each publication and the corresponding PCE value measured under 1 sun irradiation.

HTM	PCE [%]	Ref.
In situ polymerization of EDOT on TiO_2 and TBP as additive	1.2×10^{-2}	[287]
In situ polymerization of EDOT on TiO_2, TBP as additive and amphiphilic ruthenium dye with long chains	0.67	[288]
PEP under different light intensity	2.5	[296]
PEP under visible light	2.62	[290]
PEDOT:PSS	2.62	[300]
Different counter anions	2.85	[293]
Anions with different perfluoroalkyl chain length	2.9	[299]
Variation of PEP time	3.0	[294]
PEP in aqueous micellar media	5.2	[297]
Fully organic dye	6.1	[138]
PEP under monochromatic light	7.1	[295]
PEDOT hybridized with graphene and graphene/PtCo alloy	8.2	[304]

The main contributions regarding PEDOT-derived materials as HTMs are summarized in **Table 2**.

5. Sustainability of Poly(3,4-ethylenedioxythiophene):Poly(styrene sulfonic acid): An Open Discussion

Among the different applications described in the previous sections about PEDOT-based compounds in DSSCs, the substitution of platinum with PEDOT:PSS is among the most diffuse and it is usually introduced as an opportunity to improve the environmental performances and reduce the cost of the final device due to the removal of the precious metal.[305] However, specific studies dealing with the sustainability evaluation for PEDOT:PSS counter electrodes in DSSCs are not present yet. In this section, we will discuss some aspects to suggest future in-depth sustainability analysis.

When dealing with the sustainability concept in the energy field, three key adjectives must be considered: Affordable, reliable, and clean.[306,307] Affordability refers to low cost, reliability is linked to the continuous and stable availability of primary sources and cleanness regards the minimization of environmental impacts.

In DSSCs, the traditional counter electrodes are made of platinum. As already briefly discussed in Section 2, this element presents three main issues from a sustainability point of view: it is costly,[308] it is a CRM[309,310] and it is correlated with degradation and stability issues, especially when used with the I-based electrolyte. In particular, the high cost threats the affordability of the apparatus, while the criticality, being related to supply and economic risk,[311] is associated to the reliability.

Although PEDOT:PSS is often presented as a cheaper solution than platinum, it is worth highlighting that the overall cost depends also on both quantities and processes adopted for electrodes fabrication. Here we show some values to discuss costs, energy requirements, and environmental impacts; these data are obtained from experimental ones[312,313] and are illustrated in **Table 3**.

Table 3. Chemicals, processes, and costs for the preparation of DSSC cathodes based on PEDOT:PSS and platinum.

PEDOT:PSS counter electrode[a]	
Reagent type	PEDOT:PSS solution, commercially available (1.3 wt% in water)
PEDOT:PSS solution (1.3 wt% in water) cost (€ kg^{-1})[b]	896
Thickness (nm)	300
Dry film density (g cm^{-3})	1.011
Deposition method	Spin coating
Material waste (%)[c]	60
PEDOT:PSS solution primary energy (MJ kg^{-1})	159
Overall cost per area (m€ cm^{-2})	5.23
Platinum counter electrode[a]	
Reagent type	H_2PtCl_6 5 mM in isopropanol (from commercially available H_2PtCl_6 8 wt% in water)
H_2PtCl_6 8 wt% in water cost (€ kg^{-1})[b]	7276
Thickness (nm)	6
Dry film density (g cm^{-3})	21.4
Deposition method	Thermal decomposition
Material waste (%)[c]	0
Pt primary energy (MJ kg^{-1})	190 000
Overall cost per area (m€ cm^{-2})	6.43

[a]Considered area: 1 cm^2; [b]Commercial; [c]Material waste is calculated on process waste without considering solvent evaporation.

Regarding quantities, we can refer to both average material thickness (6 nm for Pt and 300 nm for PEDOT:PSS) and eventual waste during the deposition process. Performing an initial calculation on materials, taking advantages of literature data[125,126,314] and commercial prices,[315] we obtained comparable costs for the cathodes made of the two different materials (see Supporting Information). However, besides materials, processes have to be carefully investigated. For instance, platinum deposition requires high temperature heating,[125,126] while PEDOT:PSS is usually deposited through the spin coating method with a consistent waste of material (60% on a lab scale) and issues in scalability. Besides materials waste, the spin coating deposition exhibits also scalability issues. Conversely, dip coating, drop coating and inkjet printing are considered to be low waste and scalable technique, but they present some control issues (e.g., thickness and homogeneity).

The employment of PEDOT:PSS is justified by the largely enhanced processability and water solubility[79] of the composite material, but it provides relatively low conductivity (0.1 to 10 S cm^{-1})[74,316] and the further doping of the organic matrix is usually required. These treatments involve the use of solvents, acids, and/or doping agents (ionic liquids, salts, CNTs) that could jeopardize the final sustainability of the device. As an example, Xia and Ouyang exploited a InI_3 solution (1 M) to enhance PEDOT:PSS conductivity,[317] but they did not consider

that indium is a CRM[318] and, according to the Royal Society of Chemistry, with the same risk of platinum.[319]

Along with the cost reduction, PEDOT:PSS is also considered as a solution to decrease the environmental impacts. A very powerful tool to analyze how a product or a service is environmentally sustainable is the LCA. It helps to evaluate the environmental impacts from either a cradle-to-gate or a cradle-to-grave approach (either from the raw materials extraction to the factory gate or from the raw materials extraction to the disposal phase,[313] respectively). Despite LCAs for DSSCs with Pt-based counter electrodes are present in literature,[313,320] similar evaluations for PEDOT:PSS-based systems are not available yet. Studies involving platinum confirm that reducing its amount in the final device leads to environmental improvements,[321] even if the precious metal that mainly affects impacts is silver. However, they did not show any comparison with PEDOT:PSS-based cathodes.

PEDOT:PSS is also used as HTM in perovskite-based devices[322] and organic PV,[323] and LCA studies were performed for these technologies. Comparing LCA studies of different devices is not accurate, but some data could be fairly extrapolated. For instance, from the work by Garcìa-Valverde et al.,[314] it is possible to get a value for the equivalent primary energy of the solution of PEDOT:PSS utilized for cathode preparation (1.3 wt% in water), that resulted to be 159 MJ kg^{-1} (see Supporting Information). Comparing this value with the primary energy for platinum element (190 000 MJ kg^{-1}, from Ecoinvent v. 2.2–2010), the difference is really huge. A correct comparison of these values needs a consideration on the amounts of exploited materials. Including the amount of total solution used for cathode preparation (PEDOT:PSS 1.3 wt% in water) and the amount of platinum contained in the H_2PtCl_6 solution, we have a more realistic idea of the energy consumption for cathode preparation. The value for platinum is higher even if the energy for its solution preparation is not included (see Supporting Information). Our preliminary calculations show lower costs and less energy requirements for PEDOT:PSS, even if process energies have not been included. However, platinum deposition requires high temperatures, while PEDOT:PSS is obtained at room temperature. Hence, from this results we might confirm that PEDOT:PSS is more sustainable than platinum as cathode for DSSCs, but further studies are necessary.

Stability is another parameter affecting the overall sustainability. Better stability means longer lifespan and lower environmental impacts due to the avoidance of resource exploitation to produce new modules and to dispose of the old ones.[321] Hence, the evaluation of cell stability with PEDOT:PSS cathode should be investigated to know if and how lifetime improvements can be achieved with respect to Pt.

Last, but not least, environmental impacts are significantly affected by the end-of-life (EoL) phase (disposal phase).[324,325] Usually, three scenarios are examined for PV modules EoL: i) Incineration, ii) landfilling, and iii) recycling. However, for emerging PV technologies, the processes are not consolidated yet. To our knowledge, the investigation of the EoL for DSSCs with PEDOT:PSS CE cathodes is not present in literature. Some information can be borrowed from studies regarding the EoL of organic PV employing PEDOT:PSS as HTM. These studies refer to HTM removal and eventual recovering through its dissolution in chlorobenzene (with possible issues due to its halogenated nature)[326,327] and a similar approach can be considered for PEDOT:PSS as cathode material in DSSCs. A critical point in the waste management is leaching and dispersion of materials.[328] In this context, it is interesting to mention the particulate PEDOT material behavior.[321] PEDOT, in its polymeric form, is non-toxic; however, particulate PEDOT materials resulted to exhibit cytotoxic effects in human lung fibroblasts and mouse macrophages.[321,328] This is important to consider as the hydrophilicity of this compound could lead to the dispersion of this material through the environment and subsequently it might become biologically available.[328]

On the other hand, platinum could be recovered through acidic treatments and electrolysis.[329] Obviously, these treatments require energy and resources and produce waste affecting the final impacts. Parisi et al. calculated the impacts for the three scenarios: the recycling one resulted the best option, but the contribution of platinum recycling was not specified.[321]

Two last considerations have to be mentioned: the source of materials and the design for recycling. Materials from renewable or recycled sources and easiness to disassembling and recycling can furtherly improve the whole device sustainability.[325,330,331] An example for Pt-based cathodes is presented in an interesting work by Charles et al., who obtained Pt-based cathodes from waste thermocouples, enhancing resource-efficiency and mitigating materials criticality issues by decoupling supply from primary production.[324]

At a first analysis, PEDOT:PSS can be considered as a promising alternative to Pt, aiming at increasing the whole sustainability of DSSCs. However, further specific investigations are necessary to reach a final conclusion. In this context, our work can be considered as a valuable starting point.

6. Conclusions

This manuscript has offered an overview of the use of PEDOT (and PEDOT-based materials) in the DSSCs field. The dual challenge of replacing the liquid electrolyte and the Pt-based counter electrode is highly ambitious, but in both cases PEDOT-based materials have been successfully demonstrated, with properly operative lab-scale devices.

The two main aspects on which the activity of the scientific community is based are the deposition method and the formulation of the PEDOT-based components. In the first case, the goal is to create the best possible interface between different cell components and this has been demonstrated with particular success when adopting PEP processes, where PEDOT can grow directly inside the cell. As regards the formulation, literature counts many mixtures in which PEDOT is combined with salts, C-based materials or other conductive polymers. Significant improvements in conductivity values have been achieved for all these systems, but—in summary—two aspects still need to be thoroughly investigated. The first concerns the sustainability of materials and processes; in fact, most of the literature articles mention the use of PEDOT as a green strategy with respect to the components traditionally adopted in DSSCs (e.g., Pt-based cathodes and liquid electrolytes based on organic solvents), but

in-depth LCA studies have never been conducted. Second, the stability of DSSCs containing PEDOT-based components has almost never been studied in depth, either by certified protocols or by aging procedures conducted in academic laboratories.

As a future outlook, if the two critical issues stated above will be successfully fixed in the forthcoming years, a reliable path toward the achievement of solid-state and Pt-free DSSCs will be opened, which would make them even more attractive for architectural integration and portable electronics. Clearly, this also pass through an exhaustive study of PEDOT impacts (in terms of costs and environmental concerns) during its production and disposal phases; nowadays, very few data are available to this purpose. Last, but not least, a comprehensive and systematic study of PEDOT-based DSSCs fabricated changing the redox mediator or the molecular sensitizer, while keeping constant the PEDOT-based counter electrode or HTM, would lead to a strong data collection to deeply understand the real potentialities of this conductive polymer in this field.

Supporting Information

Supporting Information is available from the Wiley Online Library or from the author.

Conflict of Interest

The authors declare no conflict of interest.

Keywords

counter electrodes, dye-sensitized solar cells, hole transporting materials, platinum, poly(3,4-ethylenedioxythiophene)

Received: January 31, 2021
Revised: April 9, 2021
Published online: May 6, 2021

[1] I. Celik, R. H. Ahangharnejhad, Z. Song, M. Heben, D. Apul, *Energies* **2020**, *13*, 4131.
[2] M. Pagliaro, F. Meneguzzo, *Chem. - Eur. J.* **2017**, *23*, 15276.
[3] G. A. Heath, T. J. Silverman, M. Kempe, M. Deceglie, D. Ravikumar, T. Remo, H. Cui, P. Sinha, C. Libby, S. Shaw, K. Komoto, K. Wambach, E. Butler, T. Barnes, A. Wade, *Nat. Energy* **2020**, *5*, 502.
[4] S. Mohanty, P. K. Patra, S. S. Sahoo, A. Mohanty, *Renewable Sustainable Energy Rev.* **2017**, *78*, 539.
[5] Y. Chen, P. P. Altermatt, D. Chen, X. Zhang, G. Xu, Y. Yang, Y. Wang, Z. Feng, H. Shen, P. J. Verlinden, *IEEE J. Photovoltaics* **2018**, *8*, 8490238.
[6] A. Naderipour, Z. Abdul-Malek, S. A. Nowdeh, H. Kamyab, A. R. Ramtin, S. Shahrokhi, J. J. Klemeš, *J. Cleaner Prod.* **2021**, *283*, 124207.
[7] G. Barbose, A. J. Satchwell, *Nat. Energy* **2020**, *5*, 750.
[8] G. M. Tina, F. B. Scavo, L. Merlo, F. Bizzarri, *Appl. Energy* **2021**, *281*, 116084.
[9] Y. He, S. Guo, J. Zhou, F. Wu, J. Huang, H. Pei, *Energy Convers. Manage.* **2021**, *229*, 113779.
[10] J. Li, S. Chen, Y. Wu, Q. Wang, X. Liu, L. Qi, X. Lu, L. Gao, *Renewable Sustainable Energy Rev.* **2021**, *137*, 110626.
[11] L. Casula, G. D'Amico, G. Masala, F. Petroni, *Lett. Spat. Resour. Sci.* **2020**, *13*, 267.
[12] Renewables 2019 – Market analysis and forecast from 2019 to 2024, https://www.iea.org/reports/renewables-2019 (accessed: January 2021).
[13] Z. Wang, W. Wei, *Energy Policy* **2017**, *107*, 437.
[14] P. A. Basore, *IEEE J. Photovoltaics* **2014**, *4*, 1477.
[15] Y. Ding, J. Yao, L. Hu, S. Dai, *Sol. Energy* **2019**, *183*, 587.
[16] L. Sheng, G. Li, W. Zhang, K. Wang, *Optik* **2019**, *184*, 90.
[17] K. Deng, Z. Liu, M. Wang, L. Li, *Adv. Funct. Mater.* **2019**, *29*, 1900830.
[18] Q. Li, W. Wan, Y. Ge, B. Wang, Y. Li, C. Wang, Y. H. Zhao, Y. Liu, *Appl. Phys. Lett.* **2019**, *114*, 101906.
[19] M. Liao, B. Shan, M. Li, *J. Phys. Chem. Lett.* **2019**, *10*, 1217.
[20] N. Mariotti, M. Bonomo, L. Fagiolari, N. Barbero, C. Gerbaldi, F. Bella, C. Barolo, *Green Chem.* **2020**, *22*, 7168.
[21] M. Grätzel, *J. Photochem. Photobiol., C* **2003**, *4*, 145.
[22] Z. Ning, Y. Fu, H. Tian, *Energy Environ. Sci.* **2010**, *3*, 1170.
[23] B. O'Regan, M. Grätzel, *Nature* **1991**, *353*, 737.
[24] N. S. Peighambardoust, S. K. Asl, R. Mohammadpour, S. K. Asl, *Sol. Energy* **2019**, *184*, 115.
[25] Z. Li, L. Yu, *Sol. Energy* **2019**, *184*, 315.
[26] R. Riaz, M. Ali, T. Maiyalagan, A. S. Anjum, S. Lee, M. J. Ko, S. H. Jeong, *Appl. Surf. Sci.* **2019**, *483*, 425.
[27] H. L. Jia, Z. J. Peng, B. Q. Gong, C. Y. Huang, M. Y. Guan, *New J. Chem.* **2019**, *43*, 5820.
[28] Y. Yu, K. A. Click, S. C. Chien, J. Sun, A. Curtze, L. C. Lin, Y. Wu, *J. Phys. Chem. C* **2019**, *123*, 8681.
[29] F. Bin, *Appl. Mech. Mater.* **2014**, *563*, 299.
[30] J. Xia, Q. Wang, M. Chen, W. Li, J. Liu, J. Chen, H. Wu, S. Fan, *Electrochim. Acta* **2019**, *307*, 422.
[31] D. Lau, N. Song, C. Hall, Y. Jiang, S. Lim, I. Perez-Wurfl, Z. Ouyang, A. Lennon, *Mater. Today Energy* **2019**, *13*, 22.
[32] R. Singh, H. W. Rhee, *Energy Storage Mater.* **2019**, *23*, 390.
[33] W. Shao, Y. Liu, K. Li, S. Zhao, G. Shao, J. K. Fang, *Sol. Energy* **2019**, *189*, 450.
[34] S. Balamurugan, S. Ganesan, *Electrochim. Acta* **2020**, *329*, 135169.
[35] A. K. Rajan, L. Cindrella, *J. Electron. Mater.* **2019**, *48*, 7647.
[36] S. G. Adhikari, A. Shamsaldeen, G. G. Andersson, *J. Chem. Phys.* **2019**, *151*, 164704.
[37] D. Giri, S. K. Raut, S. K. Patra, *Dyes Pigm.* **2019**, *174*, 108032.
[38] B. M. Ali, K. A. Kumar, *ChemistrySelect* **2019**, *4*, 12983.
[39] H. L. Jia, S. S. Li, B. Q. Gong, L. Gu, Z. L. Bao, M. Y. Guan, *Sustainable Energy Fuels* **2019**, *4*, 347.
[40] F. Bella, S. De Luca, L. Fagiolari, D. Versaci, J. Amici, C. Francia, S. Bodoardo, *Nanomaterials* **2021**, *11*, 810.
[41] A. Massaro, A. B. Muñoz-García, P. Maddalena, F. Bella, G. Meligrana, C. Gerbaldi, M. Pavone, *Nanoscale Adv.* **2020**, *2*, 2745.
[42] A. Dokouzis, F. Bella, K. Theodosiou, C. Gerbaldi, G. Leftheriotis, *Mater. Today Energy* **2020**, *15*, 100365.
[43] G. Piana, M. Ricciardi, F. Bella, R. Cucciniello, A. Proto, C. Gerbaldi, *Chem. Eng. J.* **2020**, *382*, 122934.
[44] E. Pulli, E. Rozzi, F. Bella, *Energy Convers. Manage.* **2020**, *219*, 112982.
[45] B. Park, J. Moon, *Procedia Comput. Sci.* **2017**, *122*, 965.
[46] O. Almora, D. Baran, G. C. Bazan, C. Berger, C. I. Cabrera, K. R. Catchpole, S. Erten-Ela, F. Guo, J. Hauch, A. W. Y. Ho-Baillie, T. J. Jacobsson, R. A. J. Janssen, T. Kirchartz, N. Kopidakis, Y. Li, M. A. Loi, R. R. Lunt, X. Mathew, M. D. McGehee, J. Min, D. B. Mitzi, M. K. Nazeeruddin, J. Nelson, A. F. Nogueira, U. W. Paetzold, N. G. Park, B. P. Rand, U. Rau, H. J. Snaith, E. Unger, et al., *Adv. Energy Mater.* **2021**, *11*, 2002774.

[47] P. P. Boix, S. Agarwala, T. M. Koh, N. Mathews, S. G. Mhaisalkar, *J. Phys. Chem. Lett.* **2015**, *6*, 898.
[48] I. Benesperi, H. Michaels, M. Freitag, *J. Mater. Chem. C* **2018**, *6*, 11903.
[49] Y. Cao, Y. Liu, S. M. Zakeeruddin, A. Hagfeldt, M. Grätzel, *Joule* **2018**, *2*, 1108.
[50] H. Michaels, M. Rinderle, R. Freitag, I. Benesperi, T. Edvinsson, R. Socher, A. Gagliardi, M. Freitag, *Chem. Sci.* **2020**, *11*, 2895.
[51] X. Chen, X. Li, P. Wei, X. Ma, Q. Yu, L. Liu, *Chin. J. Catal.* **2020**, *41*, 435.
[52] X. Zhao, D. Wang, S. Liu, Z. Li, J. Meng, Y. Ran, Y. Zhang, L. Li, *Mater. Res. Bull.* **2020**, *125*, 110800.
[53] M. Li, C. Wang, Z. Chen, K. Xu, J. Lu, *Chem. Rev.* **2020**, *120*, 6783.
[54] S. Venkatesan, I. P. Liu, C. M. T. Shan, H. Teng, Y. L. Lee, *Chem. Eng. J.* **2020**, *394*, 124954.
[55] H. T. Chen, Y. J. Huang, C. T. Li, C. P. Lee, J. T. Lin, K. C. Ho, *ACS Sustainable Chem. Eng.* **2020**, *8*, 5251.
[56] D. Tang, R. Zhao, J. Xie, K. Zhou, Y. Han, X. Wu, H. Wu, G. Diao, M. Chen, *J. Alloys Compd.* **2020**, *829*, 154526.
[57] C. Zhou, D. Li, Y. Tan, Y. Ke, S. Wang, Y. Zhou, G. Liu, S. Wu, J. Peng, A. Li, S. Li, S. H. Chan, S. Magdassi, Y. Long, *Adv. Opt. Mater.* **2020**, *8*, 2000013.
[58] N. Zink-Lorre, E. Font-Sanchis, Á. Sastre-Santos, F. Fernández-Lázaro, *Chem. Commun.* **2020**, *56*, 3824.
[59] S. A. Hashemi, S. Ramakrishna, A. G. Aberle, *Energy Environ. Sci.* **2020**, *13*, 685.
[60] I. Y. Y. Bu, *Optik* **2020**, *217*, 164868.
[61] D. Wang, S. H. Lee, J. Kim, C. B. Park, *ChemSusChem* **2020**, *13*, 2807.
[62] F. Yang, Z. Ke, Z. Li, M. Patrick, Z. Abboud, N. Yamamoto, X. Xiao, J. Gu, *ChemSusChem* **2020**, *13*, 3391.
[63] L. Li, D. Y. Wang, Y. Y. Shan, J. J. Xie, H.-R. Tang, J. X. Chen, Y. N. Li, Q. Zhao, *Chin. J. Inorg. Chem.* **2020**, *36*, 681.
[64] L. P. Teo, M. H. Buraidah, A. K. Arof, *Ionics* **2020**, *26*, 4215.
[65] A. Aslam, U. Mehmood, M. H. Arshad, A. Ishfaq, J. Zaheer, A. U. H. Khan, M. Sufyan, *Sol. Energy* **2020**, *207*, 874.
[66] M. Wu, T. Ma, *ChemSusChem* **2012**, *5*, 1343.
[67] E. Meyer, A. Bede, N. Zingwe, R. Taziwa, *Materials* **2019**, *12*, 1980.
[68] S. Yun, P. D. Lund, A. Hinsch, *Energy Environ. Sci.* **2015**, *8*, 3495.
[69] N. Wang, J. Hu, L. Gao, T. Ma, *J. Electron. Mater.* **2020**, *49*, 7085.
[70] H. Iftikhar, G. G. Sonai, S. G. Hashmi, A. F. Nogueira, P. D. Lund, *Materials* **2019**, *12*, 1998.
[71] Y. Li, H. Shen, Y. Liu, W. Wang, H. Yuan, H. Xie, *Mater. Rev.* **2017**, *31*, 19.
[72] G. Heywang, F. Jonas, *Adv. Mater.* **1992**, *4*, 116.
[73] Y. Xu, Y. Jia, P. Liu, Q. Jiang, D. Hu, Y. Ma, *Chem. Eng. J.* **2021**, *404*, 126552.
[74] Z. Rahimzadeh, S. M. Naghib, Y. Zare, K. Y. Rhee, *J. Mater. Sci.* **2020**, *55*, 7575.
[75] M. N. Gueye, A. Carella, J. Faure-Vincent, R. Demadrille, J. P. Simonato, *Prog. Mater. Sci.* **2020**, *108*, 100616.
[76] Y. Yang, H. Deng, Q. Fu, *Mater. Chem. Front.* **2020**, *4*, 3130.
[77] N. Sultana, H. C. Chang, S. Jefferson, D. E. Daniels, *J. Pharm. Invest.* **2020**, *50*, 437.
[78] S. Panigrahy, B. Kandasubramanian, *Eur. Polym. J.* **2020**, *132*, 109726.
[79] Y. Wen, J. Xu, *J. Polym. Sci., Part A: Polym. Chem.* **2017**, *55*, 1121.
[80] S. Kirchmeyer, K. Reuter, *J. Mater. Chem.* **2005**, *15*, 2077.
[81] D. Fichou, *Handbook of Oligo- and Polythiophenes*, Wiley-VCH, Weinheim **1999**.
[82] E. W. Fager, *J. Am. Chem. Soc.* **1945**, *67*, 2217.
[83] L. Zhan, Z. Song, J. Zhang, J. Tang, H. Zhan, Y. Zhou, C. Zhan, *Electrochim. Acta* **2008**, *53*, 8319.
[84] F. Jonas, L. Schrader, *Synth. Met.* **1991**, *41*, 831.
[85] F. Von Kieseritzky, F. Allared, E. Dahlstedt, J. Hellberg, *Tetrahedron Lett.* **2004**, *45*, 6049.
[86] T. Yamamoto, A. Morita, Y. Miyazaki, T. Maruyama, H. Wakayama, Z. H. Zhou, Y. Nakamura, T. Kanbara, S. Sasaki, K. Kubota, *Macromolecules* **1992**, *25*, 1214.
[87] T. Yamamoto, M. Abla, *Synth. Met.* **1999**, *100*, 237.
[88] T. Yamamoto, *Bull. Chem. Soc. Jpn.* **1999**, *72*, 621.
[89] A. Carella, R. Centore, F. Borbone, M. Toscanesi, M. Trifuoggi, F. Bella, C. Gerbaldi, S. Galliano, E. Schiavo, A. Massaro, A. B. Muñoz-García, M. Pavone, *Electrochim. Acta* **2018**, *292*, 805.
[90] D. Pugliese, A. Lamberti, F. Bella, A. Sacco, S. Bianco, E. Tresso, *Org. Electron.* **2014**, *15*, 3715.
[91] D. Pugliese, F. Bella, V. Cauda, A. Lamberti, A. Sacco, E. Tresso, S. Bianco, *ACS Appl. Mater. Interfaces* **2013**, *5*, 11288.
[92] J. Wu, Z. Lan, J. Lin, M. Huang, Y. Huang, L. Fan, G. Luo, *Chem. Rev.* **2015**, *115*, 2136.
[93] M. I. H. A. Sohaimy, M. I. N. M. Isa, *Polymers* **2020**, *12*, 2487.
[94] G. B. M. M. Nishshanke, B. D. K. K. Thilakarathna, I. Albinsson, B. E. Mellander, T. M. W. J. Bandara, *J. Solid State Electrochem.* **2020**, *25*, 707.
[95] J. Zou, Q. Yan, C. Li, Y. Lu, Z. Tong, Y. Xie, *ACS Appl. Mater. Interfaces* **2020**, *12*, 57017.
[96] P. Karthika, S. Ganesan, A. Thomas, T. M. Sheeba Rani, M. Prakash, *Electrochim. Acta* **2019**, *298*, 237.
[97] I. P. Liu, Y. Y. Chen, Y. S. Cho, L. W. Wang, C. Y. Chien, Y. L. Lee, *J. Power Sources* **2021**, *482*, 228962.
[98] J. Cong, X. Yang, L. Kloo, L. Sun, *Energy Environ. Sci.* **2012**, *5*, 9180.
[99] M. Bidikoudi, L. F. Zubeir, P. Falaras, *J. Mater. Chem. A* **2014**, *2*, 15326.
[100] Z. Yu, N. Vlachopoulos, M. Gorlov, L. Kloo, *Dalton Trans.* **2011**, *40*, 10289.
[101] P. Mariani, A. Agresti, L. Vesce, S. Pescetelli, A. L. Palma, F. Tomarchio, P. Karagiannidis, A. C. Ferrari, A. Di Carlo, *ACS Appl. Energy Mater.* **2021**, *4*, 98.
[102] M. Ye, X. Wen, M. Wang, J. Iocozzia, N. Zhang, C. Lin, Z. Lin, *Mater. Today* **2015**, *18*, 155.
[103] Y. M. Hailu, M. T. Nguyen, J. C. Jiang, *Phys. Chem. Chem. Phys.* **2020**, *22*, 26410.
[104] K. Miettunen, J. Etula, T. Saukkonen, S. Jouttijärvi, J. Halme, J. Romu, P. Lund, *Prog. Photovoltaics* **2015**, *23*, 1045.
[105] H. Tian, L. Sun, *J. Mater. Chem.* **2011**, *21*, 10592.
[106] F. Bella, S. Galliano, C. Gerbaldi, G. Viscardi, *Energies* **2016**, *9*, 384.
[107] A. Kamppinen, K. Aitola, A. Poskela, K. Miettunen, P. D. Lund, *Electrochim. Acta* **2020**, *335*, 135652.
[108] J. H. Yum, E. Baranoff, F. Kessler, T. Moehl, S. Ahmad, T. Bessho, A. Marchioro, E. Ghadiri, J. E. Moser, C. Yi, M.d. K. Nazeeruddin, M. Grätzel, *Nat. Commun.* **2012**, *3*, 631.
[109] A. H. Tkaczyk, A. Bartl, A. Amato, V. Lapkovskis, M. Petranikova, *J. Phys. D: Appl. Phys.* **2018**, *51*, 203001.
[110] Y. Ren, N. Flores-Díaz, D. Zhang, Y. Cao, J. D. Decoppet, G. C. Fish, J. E. Moser, S. M. Zakeeruddin, P. Wang, A. Hagfeldt, M. Grätzel, *Adv. Funct. Mater.* **2020**, *30*, 2004804.
[111] H. Jiang, Y. Ren, W. Zhang, Y. Wu, E. C. Socie, B. I. Carlsen, J. E. Moser, H. Tian, S. M. Zakeeruddin, W. H. Zhu, M. Grätzel, *Angew. Chem., Int. Ed.* **2020**, *59*, 9324.
[112] Y. Zhang, Z. Sun, C. Shi, F. Yan, *RSC Adv.* **2016**, *6*, 70460.
[113] Y. Saygili, M. Stojanovic, H. S. Kim, J. Teuscher, R. Scopelliti, M. Freitag, S. M. Zakeeruddin, J. E. Moser, M. Grätzel, A. Hagfeldt, *J. Phys. Chem. C* **2020**, *124*, 7071.
[114] A. Mahmood, *J. Energy Chem.* **2015**, *24*, 686.
[115] J. L. Storck, T. Grothe, M. Dotter, S. Adabra, M. Surjawidjaja, B. Brockhagen, *Polymers* **2020**, *12*, 3035.
[116] F. Bella, A. Chiappone, J. R. Nair, G. Meligrana, C. Gerbaldi, *Chem. Eng. Trans.* **2014**, *41*, 211.

[117] G. B. M. M. M. Nishshanke, A. K. Arof, T. M. W. J. Bandara, *Ionics* **2020**, *26*, 3685.
[118] F. Bella, E. D. Ozzello, A. Sacco, S. Bianco, R. Bongiovanni, *Int. J. Hydrogen Energy* **2014**, *39*, 3036.
[119] S. Venkatesan, Y. L. Lee, *Coord. Chem. Rev.* **2017**, *353*, 58.
[120] R. A. A. Talip, W. Z. N. Yahya, M. A. Bustam, *Sustainability* **2020**, *12*, 7598.
[121] S. A. Abrol, C. Bhargava, P. K. Sharma, *Mater. Res. Express* **2020**, *7*, 106202.
[122] R. Shanti, F. Bella, Y. S. Salim, S. Y. Chee, S. Ramesh, K. Ramesh, *Mater. Des.* **2016**, *108*, 560.
[123] F. Bella, A. Verna, C. Gerbaldi, *Mater. Sci. Semicond. Process.* **2018**, *73*, 92.
[124] F. Bella, A. Lamberti, S. Bianco, E. Tresso, C. Gerbaldi, C. F. Pirri, *Adv. Mater. Technol.* **2016**, *1*, 1600002.
[125] L. Fagiolari, M. Bonomo, A. Cognetti, G. Meligrana, C. Gerbaldi, C. Barolo, F. Bella, *ChemSusChem* **2020**, *13*, 6562.
[126] S. Galliano, F. Bella, M. Bonomo, G. Viscardi, C. Gerbaldi, G. Boschloo, C. Barolo, *Nanomaterials* **2020**, *10*, 1585.
[127] M. Khalili, M. Abedi, H. S. Amoli, S. A. Mozaffari, *Carbohydr. Polym.* **2017**, *175*, 1.
[128] M. Imperiyka, A. Ahmad, S. A. Hanifah, F. Bella, *Phys. B* **2014**, *450*, 151.
[129] A. Sacco, F. Bella, S. De La Pierre, M. Castellino, S. Bianco, R. Bongiovanni, C. F. Pirri, *ChemPhysChem* **2015**, *16*, 960.
[130] S. Suriyakumar, S. Gopi, M. Kathiresan, S. Bose, E. B. Gowd, J. R. Nair, N. Angulakshmi, G. Meligrana, F. Bella, C. Gerbaldi, A. M. Stephan, *Electrochim. Acta* **2018**, *285*, 355.
[131] N. N. M. Radzir, S. A. Hanifah, A. Ahmad, N. H. Hassan, F. Bella, *J. Solid State Electrochem.* **2015**, *19*, 3079.
[132] M. Falco, L. Castro, J. R. Nair, F. Bella, F. Bardé, G. Meligrana, C. Gerbaldi, *ACS Appl. Energy Mater.* **2019**, *2*, 1600.
[133] M. Falco, C. Simari, C. Ferrara, J. R. Nair, G. Meligrana, F. Bella, I. Nicotera, P. Mustarelli, M. Winter, C. Gerbaldi, *Langmuir* **2019**, *35*, 8210.
[134] G. Piana, F. Bella, F. Geobaldo, G. Meligrana, C. Gerbaldi, *J. Energy Storage* **2019**, *26*, 100947.
[135] J. R. Nair, F. Colò, A. Kazzazi, M. Moreno, D. Bresser, R. Lin, F. Bella, G. Meligrana, S. Fantini, E. Simonetti, G. B. Appetecchi, S. Passerini, C. Gerbaldi, *J. Power Sources* **2019**, *412*, 398.
[136] M. M. Szindler, M. Szindler, L. A. Dobrzański, *Open Phys.* **2017**, *15*, 1022.
[137] S. Li, L. Qiu, C. Shi, X. Chen, F. Yan, *Adv. Mater.* **2014**, *26*, 1266.
[138] X. Liu, W. Zhang, S. Uchida, L. Cai, B. Liu, S. Ramakrishna, *Adv. Mater.* **2010**, *22*, E150.
[139] I. Chung, B. Lee, J. He, R. P. H. Chang, M. G. Kanatzidis, *Nature* **2012**, *485*, 486.
[140] B. Gao, J. Meng, *Sol. Energy* **2020**, *211*, 1223.
[141] H. Katouah, N. M. El-Metwaly, *React. Funct. Polym.* **2021**, *159*, 104810.
[142] W. Zhang, Y. Cheng, X. Yin, B. Liu, *Macromol. Chem. Phys.* **2011**, *212*, 15.
[143] C. Y. Hsu, Y. C. Chen, R. Y. Y. Lin, K. C. Ho, J. T. Lin, *Phys. Chem. Chem. Phys.* **2012**, *14*, 14099.
[144] Critical Raw Materials Alliance, https://www.crmalliance.eu/critical-raw-materials (accessed: January 2021).
[145] Z. Jin, M. Zhang, M. Wang, C. Feng, Z. S. Wang, *Acc. Chem. Res.* **2017**, *50*, 895.
[146] G. R. Li, J. Song, G. L. Pan, X. P. Gao, *Energy Environ. Sci.* **2011**, *4*, 1680.
[147] H. Wang, Y. H. Hu, *Energy Environ. Sci.* **2012**, *5*, 8182.
[148] K. Suzuki, M. Yamaguchi, M. Kumagai, S. Yanagida, *Chem. Lett.* **2003**, *32*, 28.
[149] M. Chen, L. L. Shao, *Chem. Eng. J.* **2016**, *304*, 629.
[150] W. Wang, X. Xu, Y. Liu, Y. Zhong, Z. Shao, *Adv. Energy Mater.* **2018**, *8*, 1800172.
[151] F. Hao, P. Dong, Q. Luo, J. Li, J. Lou, H. Lin, *Energy Environ. Sci.* **2013**, *6*, 2003.
[152] M. N. Lu, C. Y. Chang, T. C. Wei, J. Y. Lin, *J. Nanomater.* **2016**, *2016*, 4742724.
[153] A. Pedico, A. Lamberti, A. Gigot, M. Fontana, F. Bella, P. Rivolo, M. Cocuzza, C. F. Pirri, *ACS Appl. Energy Mater.* **2018**, *1*, 4440.
[154] M. N. Mustafa, S. Shafie, Z. Zainal, Y. Sulaiman, *Mater. Des.* **2017**, *136*, 249.
[155] A. Thess, R. Lee, P. Nikolaev, H. Dai, P. Petit, J. Robert, C. Xu, Y. H. Lee, S. G. Kim, A. G. Rinzler, D. T. Colbert, G. E. Scuseria, D. Tománek, J. E. Fischer, R. E. Smalley, *Science* **1996**, *273*, 483.
[156] S. M. Cha, G. Nagaraju, S. C. Sekhar, L. K. Bharat, J. S. Yu, *J. Colloid Interface Sci.* **2018**, *513*, 843.
[157] D. Y. Chung, Y. J. Son, J. M. Yoo, J. S. Kang, C. Y. Ahn, S. Park, Y. E. Sung, *ACS Appl. Mater. Interfaces* **2017**, *9*, 41303.
[158] Z. Qiu, Y. Wang, X. Bi, T. Zhou, J. Zhou, J. Zhao, Z. Miao, W. Yi, P. Fu, S. Zhuo, *J. Power Sources* **2018**, *376*, 82.
[159] H. H. Gong, S. H. Park, S. S. Lee, S. C. Hong, *Int. J. Precis. Eng. Manuf.* **2014**, *15*, 1193.
[160] Z. Ku, X. Li, G. Liu, H. Wang, Y. Rong, M. Xu, L. Liu, M. Hu, Y. Yang, H. Han, *J. Mater. Chem. A* **2013**, *1*, 237.
[161] P. Li, Q. Tang, *J. Power Sources* **2016**, *317*, 43.
[162] K. Subalakshmi, K. A. Kumar, O. P. Paul, S. Saraswathy, A. Pandurangan, J. Senthilselvan, *Sol. Energy* **2019**, *193*, 507.
[163] D. Vikraman, S. A. Patil, S. Hussain, N. Mengal, S. H. Jeong, J. Jung, H. J. Park, H. S. Kim, H. S. Kim, *J. Ind. Eng. Chem.* **2019**, *69*, 379.
[164] T. K. Trinh, V. T. H. Pham, N. T. N. Truong, C. D. Kim, C. Park, *J. Cryst. Growth* **2017**, *461*, 53.
[165] K. Zhang, M. W. Khan, X. Zuo, Q. Yang, H. Tang, M. Wu, G. Li, *Electrochim. Acta* **2019**, *307*, 64.
[166] M. Lickleder, G. Cha, R. Hahn, P. Schmuki, *J. Electrochem. Soc.* **2019**, *166*, H3009.
[167] T. Jeong, S. Y. Ham, B. Koo, P. Lee, Y. S. Min, J. Y. Kim, M. J. Ko, *J. Ind. Eng. Chem.* **2019**, *80*, 106.
[168] K. A. Kumar, A. Pandurangan, S. Arumugam, M. Sathiskumar, *Sci. Rep.* **2019**, *9*, 1228.
[169] T. Van Nguyen, N. T. N. Truong, P. Ho, T. K. Trinh, J. H. Kim, C. Park, *J. Mater. Sci.: Mater. Electron.* **2019**, *30*, 19752.
[170] R. N. Hanson, R. W. Giese, M. A. Davis, S. M. Costello, R. N. Hanson, M. A. Davis, *J. Med. Chem.* **1978**, *21*, 496.
[171] D. K. Kumar, S. R. Popuri, S. K. Swami, O. R. Onuoha, J. W. Bos, B. Chen, N. Bennett, H. M. Upadhyaya, *Sol. Energy* **2019**, *190*, 28.
[172] Q. S. Jiang, W. Li, J. Wu, W. Cheng, J. Zhu, T. Zhu, S. Ren, Y. Zhang, *J. Electroanal. Chem.* **2019**, *852*, 113522.
[173] F. Y. Kuo, F. S. Lin, M. H. Yeh, M. S. Fan, L. Y. Hsiao, J. J. Lin, R. J. Jeng, K. C. Ho, *ACS Appl. Mater. Interfaces* **2019**, *11*, 25090.
[174] M. Bonomo, D. Dini, *Energies* **2016**, *9*, 373.
[175] Periodic table, https://periodictable.com/Elements/029/index.html (accessed: January 2021).
[176] A. H. Alami, B. Rajab, J. Abed, M. Faraj, A. A. Hawili, H. Alawadhi, *Energy* **2019**, *174*, 526.
[177] S. Yun, X. Zhou, Y. Zhang, C. Wang, Y. Hou, *Electrochim. Acta* **2019**, *309*, 371.
[178] Q. Yang, X. Zuo, J. Yao, K. Zhang, H. Zhang, M. W. Khan, W. Wang, H. Tang, M. Wu, G. Li, S. Jin, *J. Electroanal. Chem.* **2019**, *844*, 34.
[179] M. Mohammadnezhad, G. S. Selopal, N. Alsayyari, R. Akilimali, F. Navarro-Pardo, Z. M. Wang, B. Stansfield, H. Zhao, F. Rosei, *J. Electrochem. Soc.* **2019**, *166*, H3065.
[180] Y. Di, Z. Xiao, Z. Zhao, G. Ru, B. Chen, J. Feng, *J. Alloys Compd.* **2019**, *788*, 198.
[181] B. Pang, Y. Shi, S. Lin, Y. Chen, J. Feng, H. Dong, H. Yang, Z. Zhao, L. Yu, L. Dong, *Mater. Res. Bull.* **2019**, *117*, 78.

[182] L. Li, X. Zhang, L. Fu, Q. Wang, S. Ji, M. Wu, H. Wang, W. Zhang, *Composites, Part B* **2019**, *173*, 107026.
[183] A. A. M. Sultan, E. Lou, P. T. Mativenga, *J. Cleaner Prod.* **2017**, *154*, 51.
[184] X. Zeng, J. A. Mathews, J. Li, *Environ. Sci. Technol.* **2018**, *52*, 4835.
[185] F. Bella, D. Pugliese, J. R. Nair, A. Sacco, S. Bianco, C. Gerbaldi, C. Barolo, R. Bongiovanni, *Phys. Chem. Chem. Phys.* **2013**, *15*, 3706.
[186] F. Bella, M. Imperiyka, A. Ahmad, *J. Photochem. Photobiol., A* **2014**, *289*, 73.
[187] R. Bhargava, T. Daeneke, S. J. Thompson, J. Lloyd, C. A. Palma, J. Reichert, J. V. Barth, L. Spiccia, U. Bach, *J. Phys. Chem. C* **2015**, *119*, 19613.
[188] F. Y. Ouyang, W. L. Tai, *Appl. Surf. Sci.* **2013**, *276*, 563.
[189] J. M. Pringle, V. Armel, M. Forsyth, D. R. MacFarlane, *Aust. J. Chem.* **2009**, *62*, 348.
[190] N. Balis, T. Makris, V. Dracopoulos, T. Stergiopoulos, P. Lianos, *J. Power Sources* **2012**, *203*, 302.
[191] T. Muto, M. Ikegami, K. Kobayashi, T. Miyasaka, *Chem. Lett.* **2007**, *36*, 804.
[192] J. M. Pringle, V. Armel, D. R. MacFarlane, *Chem. Commun.* **2010**, *46*, 5367.
[193] S. Ahmad, J.-H. Yum, Z. Xianxi, M. Grätzel, H.-J. Butt, M. K. Nazeeruddin, *J. Mater. Chem.* **2010**, *20*, 1654.
[194] Y. M. Xiao, J. Y. Lin, J. H. Wu, S. Y. Tai, G. T. Yue, *Electrochim. Acta* **2012**, *83*, 221.
[195] M. Gao, Y. Xu, Y. Bai, S. Jin, *Appl. Surf. Sci.* **2014**, *289*, 145.
[196] S. H. Park, O. H. Kim, J. S. Kang, K. J. Lee, J. W. Choi, Y. H. Cho, Y. E. Sung, *Electrochim. Acta* **2014**, *137*, 661.
[197] X. Yin, F. Wu, N. Fu, J. Han, D. Chen, P. Xu, M. He, Y. Lin, *ACS Appl. Mater. Interfaces* **2013**, *5*, 8423.
[198] D. H. Kim, S. E. Atanasov, P. Lemaire, K. Lee, G. N. Parsons, *ACS Appl. Mater. Interfaces* **2015**, *7*, 3866.
[199] H. Ellis, N. Vlachopoulos, L. Häggman, C. Perruchot, M. Jouini, G. Boschloo, A. Hagfeldt, *Electrochim. Acta* **2013**, *107*, 45.
[200] L. Chen, J. Jin, X. Shu, J. Xia, *J. Power Sources* **2014**, *248*, 1234.
[201] C. T. T. Thuy, D. W. Kim, S. Thogiti, H. J. Jo, J. H. Kim, R. Cheruku, *Mol. Cryst. Liq. Cryst.* **2017**, *653*, 91.
[202] R. Trevisan, M. Döbbelin, P. P. Boix, E. M. Barea, R. Tena-Zaera, I. Mora-Seró, J. Bisquert, *Adv. Energy Mater.* **2011**, *1*, 781.
[203] T. H. Lee, K. Do, Y. W. Lee, S. S. Jeon, C. Kim, J. Ko, S. S. Im, *J. Mater. Chem.* **2012**, *22*, 21624.
[204] N. Jeon, D. K. Hwang, Y. S. Kang, S. S. Im, D.-W. Kim, *Electrochem. Commun.* **2013**, *34*, 1.
[205] H. Li, Y. Xiao, G. Han, W. Hou, *J. Power Sources* **2017**, *342*, 709.
[206] S. J. Thompson, J. M. Pringle, X. L. Zhang, Y.-B. Cheng, *J. Phys. D: Appl. Phys.* **2013**, *46*, 024007.
[207] X. Xia, W. Wu, J. Ma, T. Liu, D. Fei, X. Liu, C. Gao, *RSC Adv.* **2015**, *5*, 15772.
[208] J. Ma, S. Qingfeng, Z. Fengbao, W. Mingxing, *Mater. Res. Bull.* **2018**, *100*, 213.
[209] P. Balraju, M. Kumar, M. S. Roy, G. D. Sharma, *Synth. Met.* **2009**, *159*, 1325.
[210] Y. K. Kim, S. H. Park, W. P. Hwang, M. H. Seo, H. W. Park, Y. W. Jang, M. R. Kim, J. K. Lee, *J. Korean Phys. Soc.* **2012**, *60*, 2049.
[211] M. Biancardo, K. West, F. C. Krebs, *J. Photochem. Photobiol., A* **2007**, *187*, 395.
[212] S. H. Park, J. U. Kim, J. K. Lee, M. R. Kim, *Mol. Cryst. Liq. Cryst.* **2007**, *471*, 113.
[213] S. S. Shenouda, I. S. Yahia, H. S. Hafez, F. Yakuphanoglu, *Mater. Res. Express* **2019**, *6*, 065004.
[214] C. S. Chou, C. S. Chou, Y. T. Kuo, C. P. Wang, *Adv. Powder Technol.* **2013**, *24*, 336.
[215] C. Yeon, S. J. Yun, J. Kim, J. W. Lim, *Adv. Electron. Mater.* **2015**, *1*, 1500121.
[216] C. H. Chiang, C.-G. Wu, *Org. Electron.* **2013**, *14*, 1769.
[217] W. C. Liu, Y. Liu, J. R. Jennings, H. Huang, Q. Wang, *J. Mater. Chem. A* **2014**, *2*, 10938.
[218] J. Xia, N. Masaki, K. Jiang, S. Yanagida, *J. Mater. Chem.* **2007**, *17*, 2845.
[219] Y. Saito, T. Kitamura, Y. Wada, S. Yanagida, *Chem. Lett.* **2002**, *10*, 1060.
[220] Y. Saito, W. Kubo, T. Kitamura, Y. Wada, S. Yanagida, *J. Photochem. Photobiol., A* **2004**, *164*, 153.
[221] Z. Li, J. Xu, L. Chen, R. Zhang, X. Yang, J. Xia, *Electrochim. Acta* **2017**, *242*, 219.
[222] H. Jiang, S. Sakurai, K. Kobayashi, *Electrochem. Solid-State Lett.* **2009**, *12*, F13.
[223] S. Sakurai, Y. Kawamata, M. Takahashi, K. Kobayashi, *J. Oleo Sci.* **2011**, *60*, 639.
[224] R. Han, S. Lu, Y. Wang, X. Zhang, Q. Wu, T. He, *Electrochim. Acta* **2015**, *173*, 796.
[225] T.-Y. Kim, W. Wei, W. Cho, S. Lee, J. Won, Y. S. Kang, *Chem. Commun.* **2015**, *51*, 16782.
[226] K. Wu, J. Ma, W. Cui, B. Ruan, M. Wu, *J. Photochem. Photobiol., A* **2017**, *340*, 29.
[227] F. Bella, L. Porcarelli, D. Mantione, C. Gerbaldi, C. Barolo, M. Grätzel, D. Mecerreyes, *Chem. Sci.* **2020**, *11*, 1485.
[228] G. Yue, J. Wu, Y. Xiao, J. Lin, M. Huang, *Electrochim. Acta* **2012**, *67*, 113.
[229] G. Yue, J. Wu, J. Lin, M. Huang, Y. Yao, L. Fan, Y. Xiao, *Front. Optoelectron. China* **2011**, *4*, 369.
[230] G. Yue, J. Wu, Y. Xiao, J. Lin, M. Huang, L. Fan, Y. Yao, *Chin. Sci. Bull.* **2013**, *58*, 559.
[231] C. Wang, X. Li, Y. Wu, S. Tan, *RSC Adv.* **2019**, *9*, 35924.
[232] S. Nagarajan, P. Sudhagar, V. Raman, W. Cho, K. S. Dhathathreyan, Y. S. Kang, *J. Mater. Chem. A* **2013**, *1*, 1048.
[233] M. Belekoukia, M. S. Ramasamy, S. Yang, X. Feng, G. Paterakis, V. Dracopoulos, C. Galiotis, P. Lianos, *Electrochim. Acta* **2016**, *194*, 110.
[234] K. Moolsarn, A. Tangtrakarn, A. Pimsawat, K. Duangsa, C. Mongkolkachit, W. Maiaugree, V. Amornkitbamrung, *Int. J. Photoenergy* **2017**, *2017*, 1064868.
[235] L. Fagiolari, F. Bella, *Energy Environ. Sci.* **2019**, *12*, 3437.
[236] F. Bonaccorso, Z. Sun, T. Hasan, A. C. Ferrari, *Nat. Photonics* **2010**, *4*, 611.
[237] H. Kim, J. H. Ahn, *Carbon* **2017**, *120*, 244.
[238] Y. Xu, H. Bai, G. Lu, C. Li, G. Shi, *J. Am. Chem. Soc.* **2008**, *130*, 5856.
[239] W. Hong, Y. Xu, G. Lu, C. Li, G. Shi, *Electrochem. Commun.* **2008**, *10*, 1555.
[240] L. Wan, B. Wang, S. Wang, X. Wang, Z. Guo, B. Dong, L. Zhao, J. Li, Q. Zhang, T. Luo, *J. Mater. Sci.* **2015**, *50*, 2148.
[241] G. Yue, J. Wu, Y. Xiao, J. Lin, M. Huang, Z. Lan, L. Fan, *Energy* **2013**, *54*, 315.
[242] C. P. Lee, C. A. Lin, T. C. Wei, M. L. Tsai, Y. Meng, C. T. Li, K. C. Ho, C. I. Wu, S. P. Lau, J. H. He, *Nano Energy* **2015**, *18*, 109.
[243] V. Gupta, N. Chaudhary, R. Srivastava, G. D. Sharma, R. Bhardwaj, S. Chand, *J. Am. Chem. Soc.* **2011**, *133*, 9960.
[244] L. A. Ponomarenko, F. Schedin, M. I. Katsnelson, R. Yang, E. W. Hill, K. S. Novoselov, A. K. Geim, *Science* **2008**, *320*, 356.
[245] J. C. Kim, M. M. Rahman, M. J. Ju, J. J. Lee, *RSC Adv.* **2018**, *8*, 19058.
[246] P. Y. Chen, C. T. Li, C. P. Lee, R. Vittal, K. C. Ho, *Nano Energy* **2015**, *12*, 374.
[247] G. H. Jeong, S. J. Kim, H. S. Ko, E. M. Han, K. H. Park, *Mol. Cryst. Liq. Cryst.* **2015**, *620*, 117.
[248] M. S. Ramasamy, A. Nikolakapoulou, D. Raptis, V. Dracopoulos, G. Paterakis, P. Lianos, *Electrochim. Acta* **2015**, *173*, 276.
[249] Y. C. Li, S. R. Jia, Z. Y. Liu, X. Q. Liu, Y. Wang, Y. Cao, X. Q. Hu, C. L. Peng, Z. Li, *J. Mater. Chem. A* **2017**, *5*, 7862.

[250] J. Ma, S. Yuan, S. Yang, H. Lu, Y. Li, *Appl. Surf. Sci.* **2018**, *440*, 8.
[251] Z. Lan, S. Gao, J. Wu, J. Lin, *J. Appl. Polym. Sci.* **2015**, *132*, 42648.
[252] X. Zhang, W. Lu, G. Zhou, Q. Li, *Adv. Mater.* **2020**, *32*, 1902028.
[253] E. M. Hofferber, J. A. Stapleton, N. M. Iverson, *J. Electrochem. Soc.* **2020**, *167*, 037530.
[254] A. J. Gillen, A. A. Boghossian, *Front. Chem.* **2019**, *7*, 612.
[255] H. J. Shin, S. S. Jeon, S. S. Im, *Synth. Met.* **2011**, *161*, 1284.
[256] G. Guan, Z. Yang, L. Qiu, X. Sun, Z. Zhang, J. Ren, H. Peng, *J. Mater. Chem. A* **2013**, *1*, 13268.
[257] J. Y. Lin, W. Y. Wang, S. W. Chou, *J. Power Sources* **2015**, *282*, 348.
[258] D. J. Yun, C. Jung, S. Byun, H. Ra, J. M. Kim, S. Lee, J. Hwang, S. H. Park, *Nanotechnology* **2018**, *29*, 395704.
[259] K. Susmitha, M. M. Kumari, M. N. Kumar, L. Giribabu, J. Theerthagiri, J. Madhavan, M. Raghavender, *J. Mater. Sci.: Mater. Electron.* **2016**, *27*, 4050.
[260] A. C. K. Reddy, M. Gurulakshmi, K. Susmitha, M. Raghavender, N. Thota, Y. P. V. Subbaiah, *J. Mater. Sci.: Mater. Electron.* **2020**, *31*, 4752.
[261] J. Zhang, X. Li, W. Guo, T. Hreid, J. Hou, H. Su, Z. Yuan, *Electrochim. Acta* **2011**, *56*, 3147.
[262] Y. Rhee, M. Ko, H. Jin, J.-H. Jin, N. K. Min, *Jpn. J. Appl. Phys.* **2014**, *53*, 08NJ02.
[263] Y. Xiao, J. Y. Lin, S. Y. Tai, S. W. Chou, G. Yue, J. Wu, *J. Mater. Chem.* **2012**, *22*, 19919.
[264] K. M. Lee, W. H. Chiu, H. Y. Wei, C. W. Hu, V. Suryanarayanan, W. F. Hsieh, K. C. Ho, *Thin Solid Films* **2010**, *518*, 1716.
[265] D. J. Yun, H. Ra, S. W. Rhee, *Renewable Energy* **2013**, *50*, 692.
[266] H. Li, Y. Xiao, G. Han, Y. Zhang, *Org. Electron.* **2017**, *50*, 161.
[267] S. Sakurai, H. Q. Jiang, M. Takahashi, K. Kobayashi, *Electrochim. Acta* **2009**, *54*, 5463.
[268] W. Maiaugree, S. Pimanpang, M. Towannang, S. Saekow, W. Jarernboon, V. Amornkitbamrung, *J. Non-Cryst. Solids* **2012**, *358*, 2489.
[269] F. Jafari, A. Behjat, A. R. Khoshroo, M. Ghoshani, *EPJ Appl. Phys.* **2015**, *69*, 20502.
[270] H. Seo, M. K. Son, N. Itagaki, K. Koga, M. Shiratani, *J. Power Sources* **2016**, *307*, 25.
[271] D. Song, M. Li, T. Wang, P. Fu, Y. Li, B. Jiang, Y. Jiang, X. Zhao, *J. Photochem. Photobiol., A* **2014**, *293*, 26.
[272] D. Song, M. Li, Y. Li, X. Zhao, B. Jiang, Y. Jiang, *ACS Appl. Mater. Interfaces* **2014**, *6*, 7126.
[273] S. Xu, Y. Luo, W. Zhong, Z. Xiao, Y. Luo, H. Ou, *J. Nanosci. Nanotechnol.* **2016**, *16*, 392.
[274] M. N. Mustafa, S. Shafie, Z. Zainal, Y. Sulaiman, *J. Nanomater.* **2017**, *2017*, 4045672.
[275] C. W. Kung, Y. H. Cheng, H. W. Chen, R. Vittal, K. C. Ho, *J. Mater. Chem. A* **2013**, *1*, 10693.
[276] M. Zheng, J. Huo, Y. Tu, J. Jia, J. Wu, Z. Lan, *RSC Adv.* **2016**, *6*, 1637.
[277] W. N. A. Wan Khalit, M. N. Mustafa, Y. Sulaiman, *Results Phys.* **2019**, *13*, 102355.
[278] H. Xu, X. Zhang, C. Zhang, Z. Liu, X. Zhou, S. Pang, X. Chen, S. Dong, Z. Zhang, L. Zhang, P. Han, X. Wang, G. Cui, *ACS Appl. Mater. Interfaces* **2012**, *4*, 1087.
[279] Y. L. Tsai, C. T. Li, T. Y. Huang, C. T. Lee, C. Y. Lin, C. W. Chu, R. Vittal, K. C. Ho, *ChemElectroChem* **2014**, *1*, 1031.
[280] P. Sudhagar, S. Nagarajan, Y. G. Lee, D. Song, T. Son, W. Cho, M. Heo, K. Lee, J. Won, Y. S. Kang, *ACS Appl. Mater. Interfaces* **2011**, *3*, 1838.
[281] W. Ding, Q. Jiang, G. Liu, L. Xu, P. Liu, J. Liu, F. Jiang, P. Liu, C. Liu, J. Xu, *2D Mater.* **2021**, *8*, 015008.
[282] Y. Liu, X. Li, E. Wang, Q. Zhong, T. Zhou, H. Chen, S. Chen, G. Lu, C. Liang, X. Peng, *Appl. Surf. Sci.* **2021**, *541*, 148371.
[283] C. T. Li, C. P. Lee, Y. Y. Li, M. H. Yeh, K. C. Ho, *J. Mater. Chem. A* **2013**, *1*, 14888.
[284] D. Song, M. Li, Y. Jiang, Z. Chen, F. Bai, Y. Li, B. Jiang, *J. Photochem. Photobiol., A* **2014**, *279*, 47.
[285] A. S. A. Ahmed, W. Xiang, X. Hu, C. Qi, I. S. Amiinu, X. Zhao, *Sol. Energy* **2018**, *173*, 1135.
[286] T. Xu, D. Kong, H. Tang, X. Qin, X. Li, A. Gurung, K. Kou, L. Chen, Q. Qiao, W. Huang, *ACS Omega* **2020**, *5*, 8687.
[287] Y. Saito, T. Kitamura, Y. Wada, S. Yanagida, *Synth. Met.* **2002**, *131*, 185.
[288] N. Fukuri, Y. Saito, W. Kubo, G. K. R. Senadeera, T. Kitamura, Y. Wada, S. Yanagida, *J. Electrochem. Soc.* **2004**, *151*, A1745.
[289] N. Fukuri, N. Masaki, T. Kitamura, Y. Wada, S. Yanagida, *J. Phys. Chem. B* **2006**, *110*, 25251.
[290] Y. Kim, Y. E. Sung, J. B. Xia, M. Lira-Cantu, N. Masaki, S. Yanagida, *J. Photochem. Photobiol., A* **2008**, *193*, 77.
[291] K. Murakoshi, R. Kogure, Y. Wada, S. Yanagida, *Chem. Lett.* **1997**, *26*, 471.
[292] Y. Saito, N. Fukuri, R. Senadeera, T. Kitamura, Y. Wada, S. Yanagida, *Electrochem. Commun.* **2004**, *6*, 71.
[293] J. Xia, N. Masaki, M. Lira-Cantu, Y. Kim, K. Jiang, S. Yanagida, *J. Am. Chem. Soc.* **2008**, *130*, 1258.
[294] A. J. Mozer, D. K. Panda, S. Gambhir, B. Winther-Jensen, G. G. Wallace, *J. Am. Chem. Soc.* **2010**, *132*, 9543.
[295] X. Liu, Y. Cheng, L. Wang, L. Cai, B. Liu, *Phys. Chem. Chem. Phys.* **2012**, *14*, 7098.
[296] B. W. Park, L. Yang, E. M. J. Johansson, N. Vlachopoulos, A. Chams, C. Perruchot, M. Jouini, G. Boschloo, A. Hagfeldt, *J. Phys. Chem. C* **2013**, *117*, 22484.
[297] J. Zhang, L. Yang, Y. Shen, B. W. Park, Y. Hao, E. M. J. Johansson, G. Boschloo, L. Kloo, E. Gabrielsson, L. Sun, A. Jarboui, C. Perruchot, M. Jouini, N. Vlachopoulos, A. Hagfeldt, *J. Phys. Chem. C* **2014**, *118*, 16591.
[298] J. Zhang, M. Pazoki, J. Simiyu, M. B. Johansson, O. Cheung, L. Häggman, E. M. J. Johansson, N. Vlachopoulos, A. Hagfeldt, G. Boschloo, *Electrochim. Acta* **2016**, *210*, 23.
[299] J. Xia, N. Masaki, M. Lira-Cantu, Y. Kim, K. Jiang, S. Yanagida, *J. Phys. Chem. C* **2008**, *112*, 11569.
[300] J. K. Lee, S. I. Jang, B. H. Jung, H. J. Choi, S. B. Lee, S. H. Park, M. R. Kim, *Mol. Cryst. Liq. Cryst.* **2009**, *505*, 175.
[301] J. Huang, P. F. Miller, J. S. Wilson, A. J. de Mello, J. C. de Mello, D. D. C. Bradley, *Adv. Funct. Mater.* **2005**, *15*, 290.
[302] C. C. Jayme, J. Kanicki, F. Kajzar, A. F. Nogueira, A. Pawlicka, *Mol. Cryst. Liq. Cryst.* **2016**, *627*, 38.
[303] C. A. Ng, D. H. Camacho, *IOP Conf. Ser.: Mater. Sci. Eng.* **2015**, *79*, 012020.
[304] Q. Li, H. Li, X. Jin, Z. Chen, *Electrochim. Acta* **2018**, *260*, 413.
[305] U. Ahmed, M. Alizadeh, N. A. Rahim, S. Shahabuddin, M. S. Ahmed, A. K. Pandey, *Sol. Energy* **2018**, *174*, 1097.
[306] Goal 7 – ensure access to affordable, reliable, sustainable and modern energy for all, https://sdgs.un.org/goals/goal7 (accessed: January 2021).
[307] Goal 7 – ensure access to affordable, reliable, sustainable and modern energy for all, https://www.un.org/en/chronicle/article/goal-7-ensure-access-affordable-reliable-sustainable-and-modern-energy-all (accessed: January 2021).
[308] Platinum price live chart by BullionVault Ltd, https://www.bullionvault.com/platinum-price-chart.do (accessed: January 2021).
[309] S. I. Hallstedt, O. Isaksson, *J. Cleaner Prod.* **2017**, *161*, 40.
[310] A. Månberger, B. Stenqvist, *Energy Policy* **2018**, *119*, 226.
[311] A. Cimprich, V. Bach, C. Helbig, A. Thorenz, D. Schrijvers, G. Sonnemann, S. B. Young, T. Sonderegger, M. Berger, *J. Ind. Ecol.* **2019**, *23*, 1226.
[312] W. Wei, H. Wang, Y. H. Hu, *Int. J. Energy Res.* **2014**, *38*, 1099.
[313] M. L. Parisi, S. Maranghi, R. Basosi, *Renewable Sustainable Energy Rev.* **2014**, *39*, 124.

[314] R. García-Valverde, J. A. Cherni, A. Urbina, *Prog. Photovoltaics* **2010**, *18*, 535.
[315] Merck KGaA, https://www.sigmaaldrich.com (accessed: January 2021).
[316] Y. H. Kim, C. Sachse, M. L. MacHala, C. May, L. Müller-Meskamp, K. Leo, *Adv. Funct. Mater.* **2011**, *21*, 1076.
[317] Y. Xia, J. Ouyang, *Org. Electron.* **2010**, *11*, 1129.
[318] L. Erdmann, T. E. Graedel, *Environ. Sci. Technol.* **2011**, *45*, 7620.
[319] Periodic table of the Royal Society of Chemistry, https://www.rsc.org/periodic-table (accessed: January 2021).
[320] M. J. De Wild-Scholten, A. C. Veltkamp, Environmental life cycle analysis of dye sensitized solar devices; status and outlook, *22nd European Photovoltaic Solar Energy Conference and Exhibition*, Milan, Italy, 3–7 September **2007**.
[321] M. L. Parisi, S. Maranghi, L. Vesce, A. Sinicropi, A. Di Carlo, R. Basosi, *Renewable Sustainable Energy Rev.* **2020**, *121*, 109703.
[322] J. Gong, S. B. Darling, F. You, *Energy Environ. Sci.* **2015**, *8*, 1953.
[323] S. Lizin, S. Van Passel, E. De Schepper, W. Maes, L. Lutsen, J. Manca, D. Vanderzande, *Energy Environ. Sci.* **2013**, *6*, 3136.
[324] R. G. Charles, P. Douglas, J. A. Baker, M. J. Carnie, J. O. Douglas, D. J. Penney, T. M. Watson, *J. Cleaner Prod.* **2018**, *202*, 1167.
[325] A. Dubreuil, S. B. Young, J. Atherton, T. P. Gloria, *Int. J. Life Cycle Assess.* **2021**, *15*, 621.
[326] J. M. Kadro, A. Hagfeldt, *Joule* **2017**, *1*, 29.
[327] B. J. Kim, D. H. Kim, S. L. Kwon, S. Y. Park, Z. Li, K. Zhu, H. S. Jung, *Nat. Commun.* **2016**, *7*, 11735.
[328] Y. S. Zimmermann, A. Schäffer, C. Hugi, K. Fent, P. F. X. Corvini, M. Lenz, *Environ. Int.* **2012**, *49*, 128.
[329] C. E. I. Latunussa, F. Ardente, G. A. Blengini, L. Mancini, *Sol. Energy Mater. Sol. Cells* **2016**, *156*, 101.
[330] J. Atherton, *Int. J. Life Cycle Assess.* **2007**, *12*, 59.
[331] G. Rebitzer, Integrating life cycle costing and life cycle assessment for managing costs and environmental impacts in supply chains, in: S. Seuring, M. Goldbach, Cost management in supply chains. Physica, Heidelberg, **2002**.

Lucia Fagiolari graduated cum laude and received her Ph.D. in Chemical Sciences from the University of Perugia, where she was involved in the synthesis and characterization of heterogeneous catalysts for water splitting applications. Currently, she works as post-doctoral researcher in the Electrochemistry Group at Politecnico di Torino. Her research concerns the development of aqueous-based DSSCs and potassium batteries, focusing on sustainable preparation strategies of innovative electrodes and electrolytes. She is author of 9 peer-reviewed papers (*h*-index 5) and is member of the Italian Chemical Society since 2015.

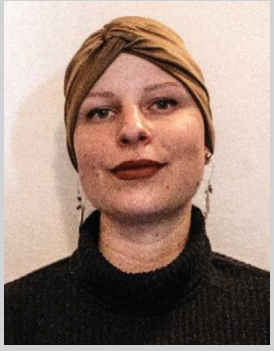

Erica Varaia graduated in Chemical and Sustainable Process Engineering at the Politecnico di Torino, focusing on chemical processes design and development. She currently works as a process engineer in a company aiming at implementing sustainability-related aspects of industrial chemistry processes. Due to her interests in environment and sustainability, she is also a volunteer for the Sea Shepherd association, that practices a direct action to investigate and act—when necessary—to prevent illegal activities in the sea.

Nicole Mariotti graduated cum laude at the University of Camerino defending a thesis on green and sustainable approaches in the synthesis of nitro-compounds. She was then enrolled in the Erasmus Traineeship Program developing green one-pot multicomponent reactions. After her Master degree, she joined the Department of Chemistry at the University of Turin, where she continued her studies attending an interdisciplinary Ph.D. course in Innovation for the Circular Economy, working on sustainable and innovative materials for energy-related application. She is coauthor of 4 peer-reviewed publications.

Matteo Bonomo is Assistant Professor in Industrial Chemistry at the University of Turin and his work is mainly related to the synthesis and characterization of innovative materials for emerging photovoltaics. More recently, he has been involved in the investigation of structural and electronic properties of Ionic Liquids and Deep Eutectic Solvents for energy application. He has received, among others, the Junior "ENERCHEM 2020" prize for his innovative contribution in Chemistry for Renewable Energy. He is coauthor of 46 publications (*h*-index 14, >500 citations) in international peer-reviewed journals.

Claudia Barolo is Associate Professor of Industrial Chemistry at the Department of Chemistry of the University of Turin. Her research interest is focused mostly on the synthesis and characterization of organic and hybrid functional materials (from molecules to polymers) able to interact with light and their possible application in energy related fields (optoelectronics, lighting and solar cells). She is also vice-coordinator of the Ph.D. Programme in Innovation for the Circular Economy at the University of Turin. Her work resulted in more than 120 publications (*h*-index 34, >3800 citations).

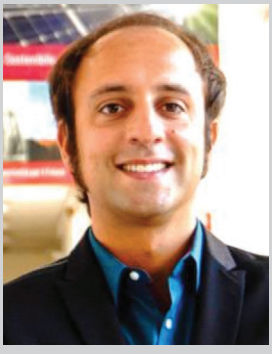

Federico Bella is Associate Professor of Principles of Chemistry for Applied Technologies at Politecnico di Torino. He works in the Electrochemistry Group, leading the research activities on hybrid photovoltaics and post-lithium batteries. He has recently received the "Environment, Sustainability & Energy Division early Career Award" from the Royal Society of Chemistry. He is author of 90 publications (*h*-index 55) and is member of the Editorial Board of Chemical Engineering Journal and ChemSusChem. He is also member of the International Relations Commission of the Italian Chemical Society. Since 2021, he leads the ERC Starting Grant "SuN_2rise" on sun-powered electrochemical nitrogen reduction.